IAEA REFERENCE DATABASE FOR BETA-DELAYED NEUTRON EMISSION EVALUATION

I.N.Borzov

National Research Centre “Kurchatov Institute”, Moscow, Russia
Bogolubov Laboratory of Theoretical Physics
Joint Institute of Nuclear Research, Dubna, Russia

Beta-decay of very neutron-rich nuclei

Self-consistent β-decay models,

RIB experiments,

Astrophysical r-process modeling.

1. Nuclear models far off stability are well guided by β-decay data on short-lived nuclei.

2. FRIB experiments need reliable predictions of β-decay properties .

3. Most of neutron-rich nuclei involved in the r-process have yet to be discovered. Predictions of β–rates are unavoidable in the modelling of the r-process.

Classical ("hot") r-process nucleosynthesis:
(n,ϒ) - (ϒ,n) equilibrium is reached.

T ~ 10(9)K ~ 100 keV
N_n ~ 10(20) cm-3
Sn ≤ 3 MeV

Neutron Capture / Photo-dissociation

$$(Z,N) + n \leftrightarrow (Z,N+1) + \gamma$$

Beta Decay

$$(Z,N) \rightarrow (Z+1,N-1) + e^- + \overline{\nu}_e$$

τ (n,ϒ) ≤ τ (β)

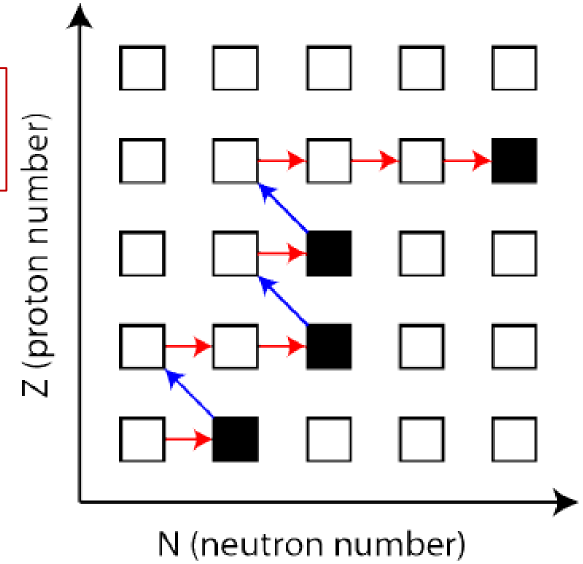

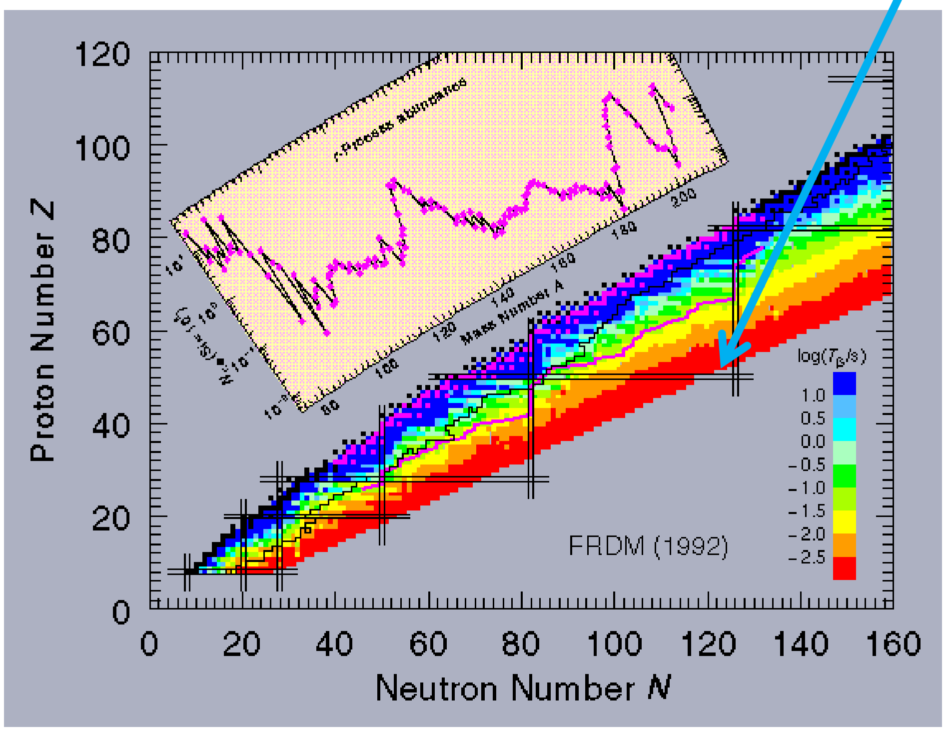

The r-process paths goes far off the stability.

Isotopes @ N=50, 82, 126 are extra-bound.
Matter flow has to "wait" for several ***beta-decays*** *to occur.*

Matter accumulates in the ***Waiting Points*** *@ N=50, 82, 126.*

Main elemental abundance peaks :
@ A=80, 130, 195

The beta-half-lives define the timescale T®, relative abundances and final abundance pattern

Astrophysical conditions: *T, Nn, S/b, Nn/Ns*

Nuclear input: *Masses (Q_β Sn…),*

Beta-decay half-lives T1/2, (n, ɣ)- cross sections

for about 2000 nuclides !

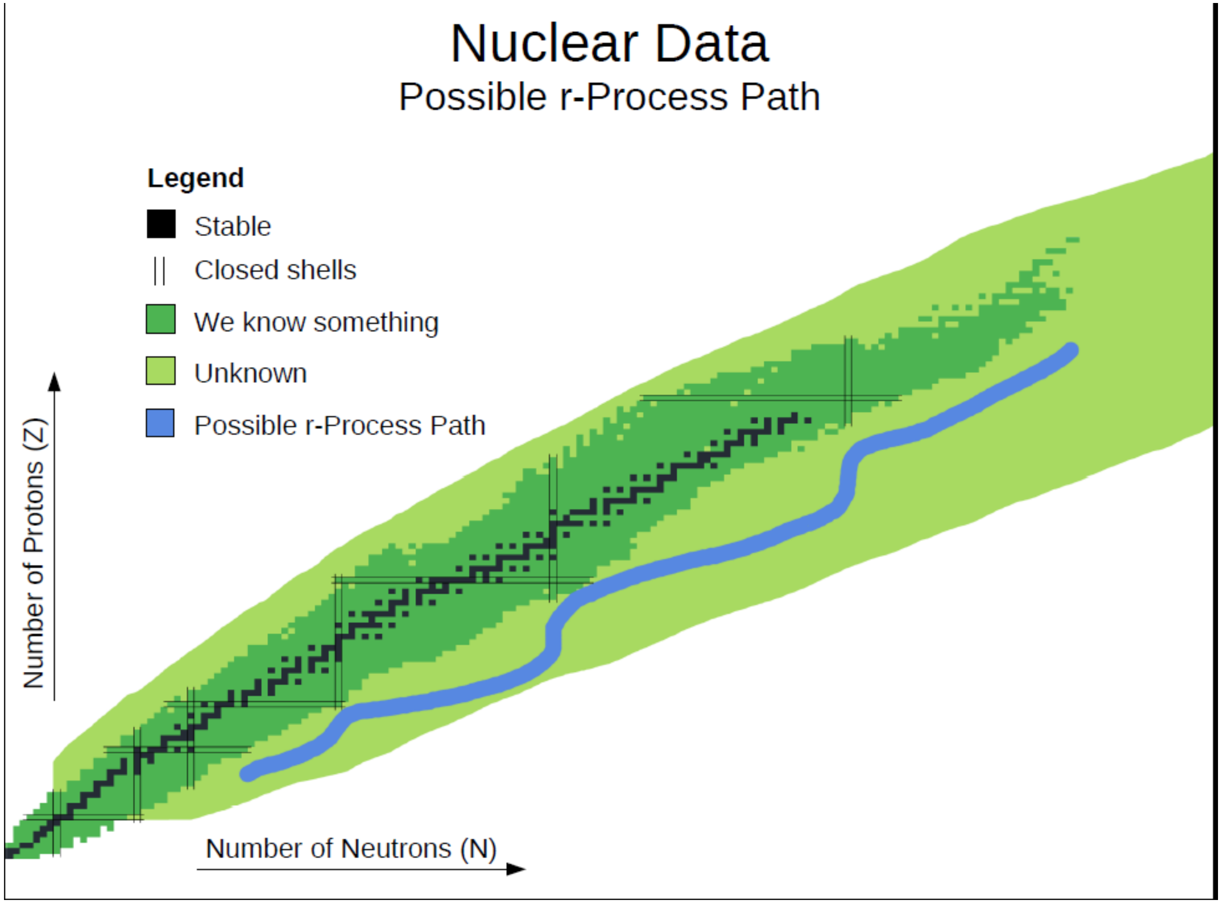

Status: Helmholtz School 2014 !

Progress has been achieved in the last 3 years.

RIKEN: EURICA and BRIKEN CAMPAIGNS (N~50, 82)

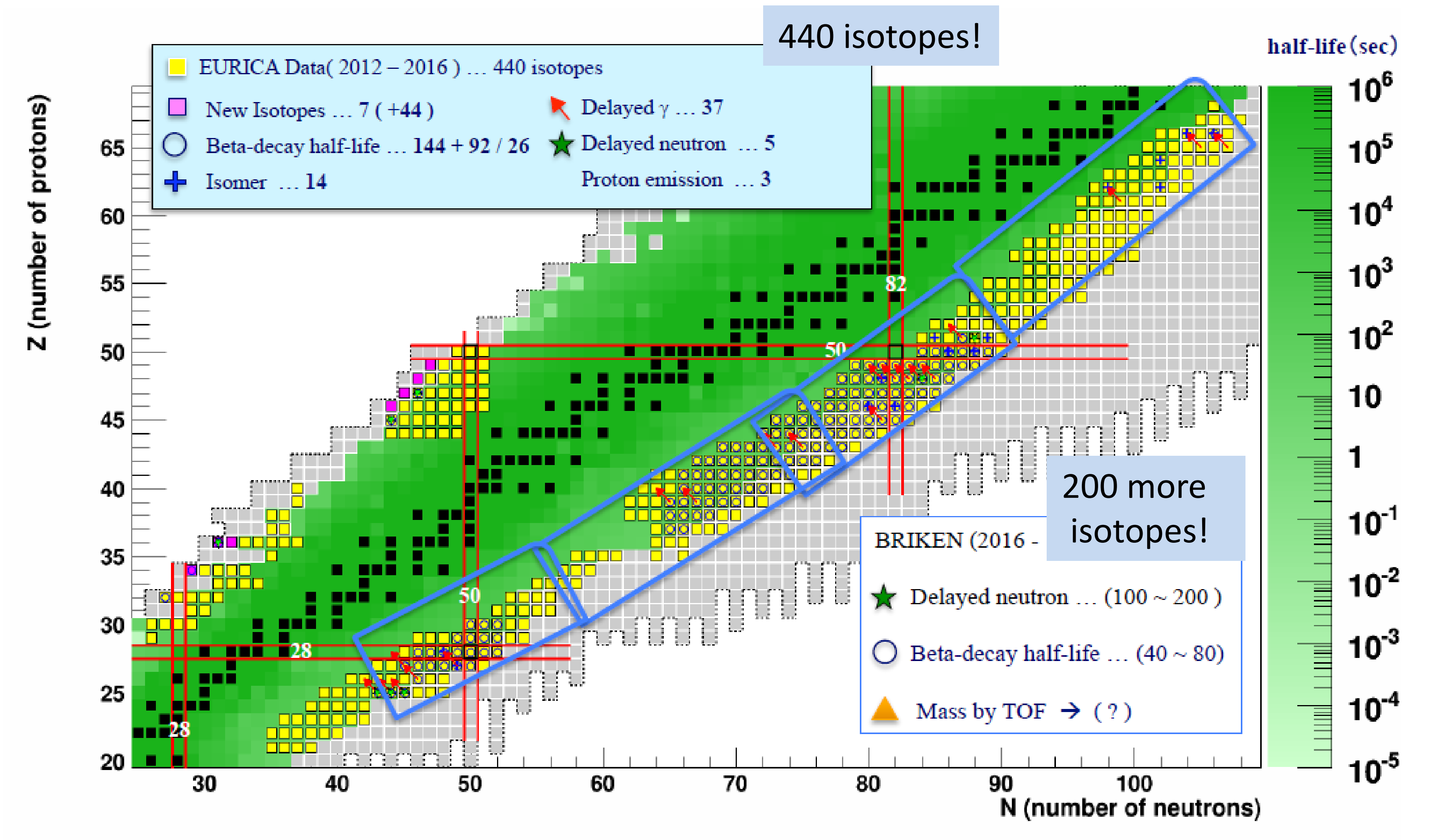

GSI-FRS (20 nuclides N~126), CERN (N~34), ORNL, JINR-ALTO , …

Outline (I) 理論系

Self-consistent approach to beta-decay.
Density functional theory is the method of choice.

GLOBAL MODELS :
Parameters are fitted to few sample nuclei and stay the same for all A

DF + Continuum QRPA
DF3- **spherical** ➔ ~300 **quasi-spherical nuclei;**

Relativistic HB + QRPA
D3C*- **spherical** ➔ **all nuclei;**

Finite Amplitude Method
Sk(yrme) O'- **deformed** ➔ **all even-even nuclei**
odd for A=80, 160

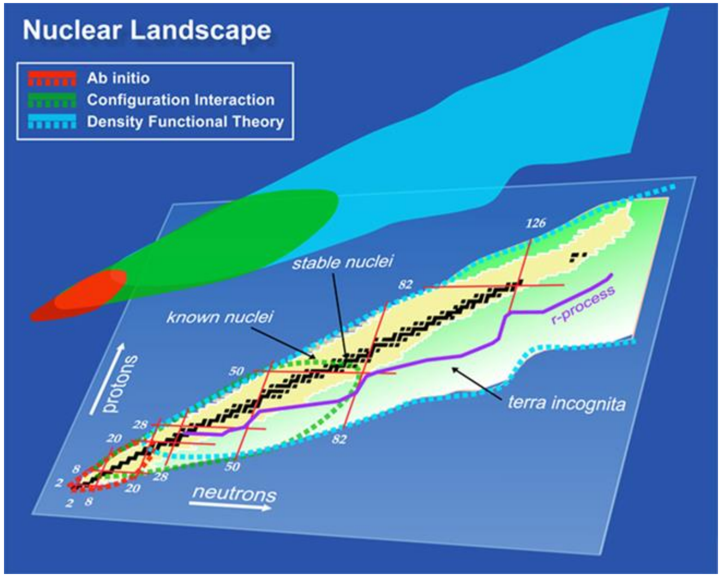

DF : Quality of the ground state description:
cf. quasi-particle energies and Q_{β}, S_{xn} values

QRPA: Reliability of β–strength functions
cf. available decay schemes and integral quantities.

Effects beyond the QRPA:

2nd-QRPA
with Quasiparticle-Phonon Coupling
(QPC)
and Shell-Model

GLOBAL SELF-CONSISTENT QRPA MODELS.
Gamow-Teller + First-Forbidden decays.

Model	The ground state (g.s.)	NN-interaction	Details
DF+CQRPA [1] $t \sim N_{ph}^2 - N_{ph}^3$	Spherical g.s **DF3,DF3a, FaNDF_0 functional.** A-dependent,density dependent δ-pairing	ph: δ-function +π + ρ meson exchange pp: Z-independent δ-function **Full ph basis** **Universal parameters**	400 **(quasi-) spherical nuclei** **No direct fitting to T1/2.**
RHB+QRPA [2] $t \sim N_{ph}^2 - N_{ph}^3$	Spherical g.s. **D3C* functional.** Relativistic Hartree-Bogolubov. Finite range pairing: Gogny D1S.	ph: D3C* pp: (N-Z)-dependent, finite range: Gogny D1S.	**All nuclei.** **Fitting to the T1/2 of the sample nuclei.**
F A M [3] ***Iterative QRPA*** $t \sim N_{ph}$!	**Spherical & Deformed g.s.** **Skyrme functional SkO'.**	ph: SkO' fitted to Landau-Migdal interaction pp: density dependent δ-function	**All even-even nuclei.** **Odd-odd , odd-A near A=80,160** **Fitting to the GT energies and T1/2 of 44 sample nuclei.**

1. I.N. Borzov., Phys. Rev. **C 67**, 025802 (2003).
2. T. Marketin, L.Huther, G. Martinez-Pinedo., Phys. Rev. **C 93**, 025805 (2015).
3. M. T. Mustonen, T. Shafer, Z. Zenginerler, J. Engel., Phys.Rev. **C 90**, 024308 (2014).
   M. T. Mustonen, J. Engel., Phys.Rev. **C 93**, 014304 (2015).
   T. Shafer, J. Engel, C. Fro:hlich, C.G. Mclaughlin, Mumpower, R. Surman. , Phys. Rev. **C 94,** 055802 (2017).

LOCAL SELF-CONSISTENT MODELS

Model	The ground state (g.s.)	NN-interaction	Details
Shell-model [1] $N_{np\text{-}nh} \leq 10^{10}$	Spherical & Deformed g.s. Self—consistent. **Fine structure of beta-strength function !**	N= 50 [35]; N= 82 [36]	Nuclei near the closed N=50,82,126 shells. **Fitting of (g_A/G_V)**
Skyrme-FRSA (pnQRPA)	Spherical g.s. Skyrme functional. BCS pairing **Quasiparticle-phonon coupling**	ph: Separabilized Skyrme + tensor interaction (T35, T44) Extension to the pp-channel is done.	Nuclei near the closed shells N= 20,28,50,82. Inclusion of FF transitions is possible

1. Q. Zhi, E. Caurier, J. Cuenca-Garc'ia, K. Langanke, G. Mart'inez-Pinedo, K. Sieja, Phys. Rev. **C87**, 025803 (2013).

PHYSICAL REVIEW C **90**, 044320 (2014)

Influence of 2p-2h configurations on β-decay rates

A. P. Severyukhin,[1] V. V. Voronov,[1] I. N. Borzov,[1] N. N. Arsenyev,[1] and Nguyen Van Giai[2]
[1]*Bogoliubov Laboratory of Theoretical Physics, Joint Institute for Nuclear Research, 141980 Dubna, Moscow region, Russia*
[2]*Institut de Physique Nucléaire, CNRS-IN2P3 and Univ. Paris-Sud, 91405 Orsay, France*
(Received 26 June 2014; published 24 October 2014)

PHYSICAL REVIEW C **95**, 034314 (2017)

Multi-neutron emission of Cd isotopes

A. P. Severyukhin,[1,2] N. N. Arsenyev,[1] I. N. Borzov,[3,1] and E. O. Sushenok[1,2]

Beta-strength function, half-life, Pn-value

$$T_{1/2} = \frac{D}{\left(\frac{G_A}{G_V}\right)^2 \int_0^{Q\beta} S_L(\omega)\ \ f_0(Z,\omega)\ \ d\omega}$$

$S_L(\omega) -\ \ \beta - strength\ \ \ function$

$D = 2\pi^3 \ln 2 / G_V{}^2 m_e{}^5 = 6163s$

$G_A / G_V = 1.26$

$$f_0(Z,A,\omega) = \int_0^{\omega} F(Z,A,\omega) pW(\omega - W)^2 dW$$

$f_0(Z,\omega) \sim \omega^5 - amplifies\ \ the$

$high-energy\ \ tail\ of\ \ S_\beta\ (\omega)!$

$$P_n = \frac{\int_{B_n(Z+1)}^{Q\beta} S_L(\omega)\ f_0(Z,\omega) P_{if}\ (j_{if}, E_n) d\omega}{\int_0^{Q\beta} S_L(\omega)\ f_0(Z,\omega) d\omega}$$

$P_{if} = \Gamma_n / (\Gamma_n + \Gamma_\gamma),$

$\Gamma_\gamma << \Gamma_n \quad \Rightarrow \quad P_{if} \approx 1$

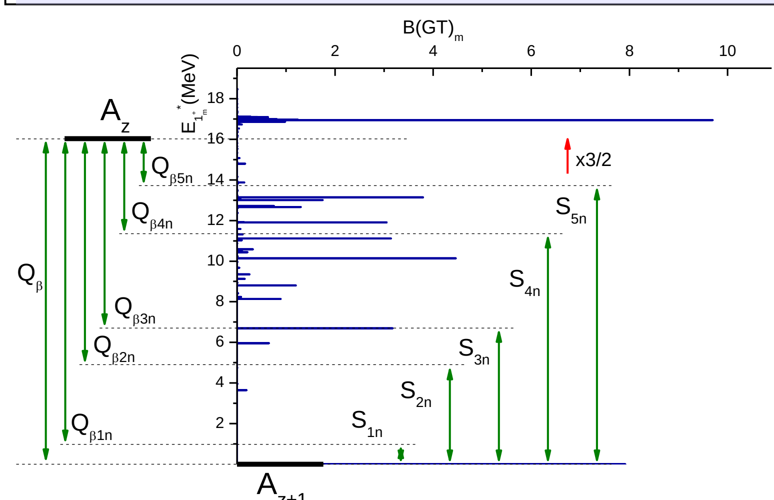

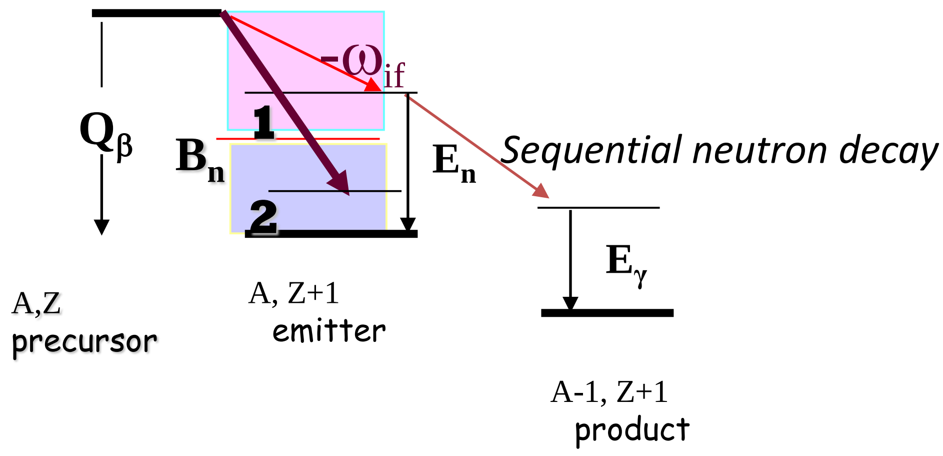

EDF. Self-Consistent Ground State

An upper limit of exact E total:

$$E[\rho,\nu] = Tr\left(\frac{p^2}{2M}\rho\right) + E_{\text{int}}[\rho,\nu]$$

$$Kohn-Sham\ quasiparticle\ local\ EDF, \quad M^* = 1$$

$$E_{\text{int}} = \sum_{main,Coul,sl} \varepsilon_n[\rho] + \frac{1}{2}\ \nu^*\ F^{\xi}[\rho]\nu$$

$$F^{\xi} - volume + surface$$

$$\boldsymbol{H} = \begin{pmatrix} \boldsymbol{h}-\boldsymbol{\mu} & -\boldsymbol{\Delta} \\ -\boldsymbol{\Delta} & \boldsymbol{\mu}-\boldsymbol{h} \end{pmatrix}$$

$$\mathbf{h} = \frac{\mathbf{p}^2}{\mathbf{2m}} + \frac{\delta \mathbf{E}}{\delta \rho} \sim \rho$$

$$\mathbf{\Delta} = \frac{\delta \mathbf{E_{int}}}{\delta \nu}$$

$$HFB-like \quad iterative \quad procedure$$

$$\rho_0, \nu_0 \Rightarrow h_0, \Delta_0 \Rightarrow \rho_1, \nu_1 \Rightarrow h_1, \Delta_1$$

DF functional by S.A. Fayans et al.

(generalization of the Skyrme functional)

DF3 S.A. Fayans, S.V. Tolokonnikov,E.Trykov, D. Zawischa, Nucl.Phys. A676 (2000) 49.
I.N. Borzov, S.A. Fayans, E. Kromer, D. Zawischa Z. Phys. A335(1996) 117

$FaNDF^0$ S.A. Fayans JETP Letters 68,169 (1998)

Fitted to the masses, specially fitted to s.p energies of very neutron-rich doubly-magic 132Sn .
FaNDF also fitted to the neutron matter EOS.

Self-Consistent Ground State . Fayans EDF.

Fayans EDF

$$\mathcal{E}(\rho) = \frac{a\rho^2}{2}\frac{1+\alpha\rho^\sigma}{1+\gamma\rho}.$$

DF

Skyrme EDF

$$E_0^{\text{int}}[\rho] = \int \mathcal{E}(\rho(\mathbf{r}))d^3r = \int \frac{a\rho^2}{2}(1+\alpha\rho^\sigma)\,d^3r,$$

Sk

At ϒ = 0 DF ρ- dependence is similar to Skyrme ansatz .

DF vs Sk

- ***Effective mass = bare mass ($m^* / M_N = 1$)***
- ***Sophisticated density – dependence of ε_{int} : linear-fractional (Pade-like) structure***
- ***Pairing DF depends on the gradient of density***

NB ! Deformed DF S.V. Tolokonnikov, I.N. Borzov, M. Kortelainen, Y.S. Lutostansky, E.E. Saperstein. J. Phys. G 42, 076102 **(2015)**

NB ! Proposal of hybrid functional ➔ *"normal part of Sk + pairing part of DF" :* P.-G. Reinhard, W. Nazarewicz. nucl-th 1704.07430 **(2017)**

Spin-isospin excitations (GT, FF).
Continuum pn-QRPA based on the generalized density-functional

S=0, T=1 (nn,pp) mass dependent g.s . paring + S=1, T=0 (pn) dynamic pairing
*Continuum **pnQRPA**, full ph-basis, **SO(8) symmetry***

Möller, P.; Nix, J. R.; Kratz, K.-L.
ADNDT, Vol. 66, p.131,1996

Pairing only in the g.s.
Dynamic pairing ignored.
BCS + RPA, SU(4) .
Spurious effects.

U: **Particle-hole channel:**
δ-interaction
with Landau-Migdal constant g'
+ π-meson + ρ-meson exchange

V: **Particle-particle channel:**
T=0, δ-interaction
with one parameter: g'_{pp}

CQRPA :
NN-interaction parameters (ph):
are the same for all nuclei with A>40.

CQRPA based on the self-consistent g.s.

$$F^{\omega}{}_{\tau\tau} = \frac{\delta^2 E}{\delta\rho^{\tau}\delta\rho^{\tau}} \qquad F^{\xi}{}_{\tau\tau} = \frac{\delta^2 E}{\delta\nu^{\tau}\delta\nu^{\tau}}$$

An impact of spin-dependent terms on nuclear masses is of order of 100KeV.
(J. Margueron et al. J.Phys.G 36(2009) 125103)

Approximation:

The spin-isospin (time-odd) parts of the effective NN-interaction are defined independently of the scalar (time-even) parts.

Generalized Finite Fermi System Theory : ***DF+CQRPA***

- *Universal (the same for all A) effective NN-interaction in the particle-hole channel* *Landau-Migdal (δ) + π-meson + ρ-meson.* *(fitted to the GTR in a single nucleus ^{208}Pb)*
- *Universal effective NN-interaction in the particle-particle channel (S=1,T=0):* *pairing-like delta interaction*
- *An advantage: full ph-basis CQRPA, the NN-interaction parameters are taken as mass-independent.*

β–decay strength functions are needed !

Integral beta-decay properties are available…

Experimental β–strength functions are incomplete. $SJ_{LS}(\omega, \Gamma^{\uparrow}, \Gamma^{\downarrow})$

Integrals over the full and partial sub-spaces help to constrain

At least T1/2 , %FF and Pxn should be analyzed together !

$T_{1/2}=ln2/\lambda$, **Pn tot** **Pxn** ,

$$\%FF = \lambda_{FF} / \lambda = (TGT - T) / TGT$$

$$\frac{T1/2}{Pn}, \quad \frac{T1/2}{Pxn} \quad \frac{P(x-1)n}{Pxn}$$

Systematics.

$\frac{T1/2}{Pn}$ *EA McCutchan, AA Sonzogni, TD Johnson, D Abriola, M Birch, B Singh*

Physical Review C 86 (4), 041305 (2012).

In this systematics , the contribution of the FF has not been accounted for !

Beta-decay near the shell-closures N=50, 82, 126.

(II) Comparison of the DF+CQRPA , RHB+CQRPA ,FAM calculations with the data on short-lived nuclei from RIB experiments

1. I.N. Borzov., Phys. Rev. **C 67**, 025802 (2003).
2. T. Marketin, L.Huther, G. Martinez-Pinedo., Phys. Rev. **C 93**, 025805 (2015).

Adequate description of the phase-space(s) is important . Q_{β}, S_{xn} are treated on equal footing with ε (q-p).

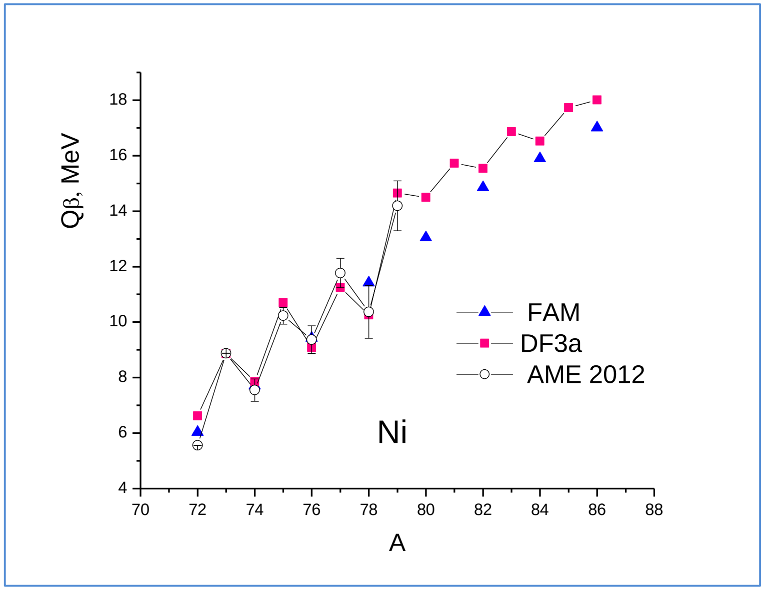

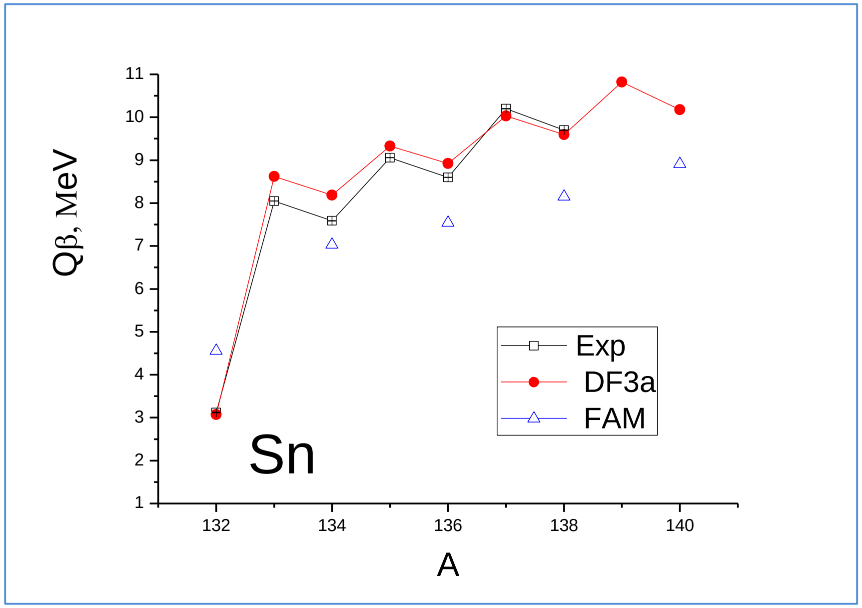

Reference Ni, Sn chains:

DF3 $|\Delta Q_{\beta}|$ is up to 0.6MeV , FAM underestimate Q_{β} up to 1.5 MeV, RHB ?

Underestimation *of the **Q_{β}** may cause distortion of the β-decay half-lives, Pn values…*

I.N.B. Phys.Rev. ***C 67*** *025802 (2003); Phys. At. Nucl.* ***79 (6)*** *921 (2016).*

DF3, DF3a functional was fitted to the experimental single-particle levels of 132Sn and 208Pb

DF3a : a possibility to fix J / π g.s. before variation.

Z<28, N < 50 REGION.
GT decays dominate for Co isotopes at A≤77 .

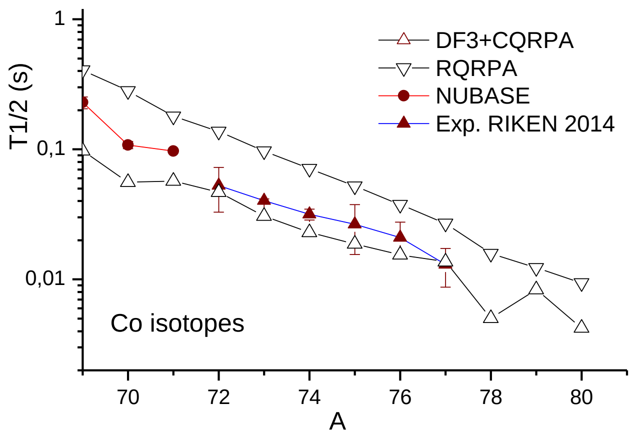

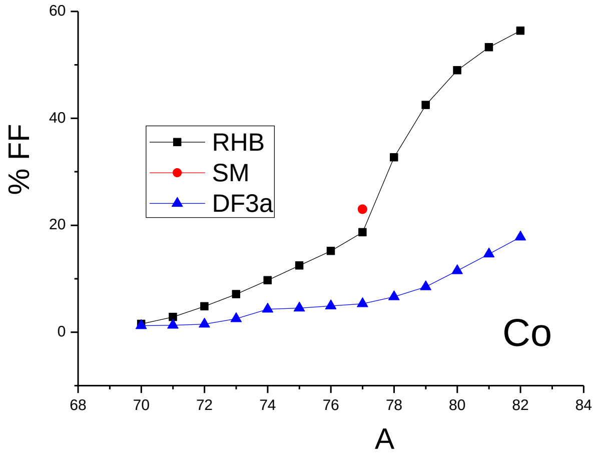

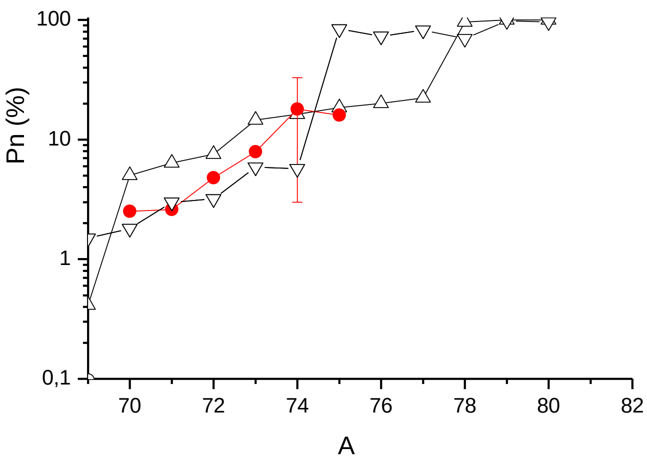

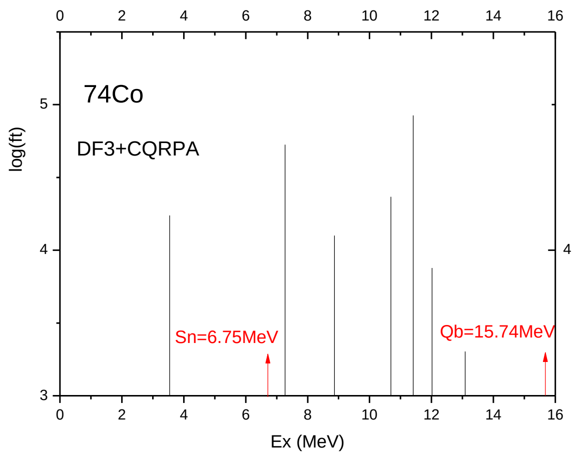

In all models (DF3, SM and RHB) at N ≤ 50 the GT decays dominate, %FF differs (DF3: 5%, RHB 18%).

N ~ 50 REGION: Comparison of T1/2 in DF3, RHB, FAM

RHB, FAM : T1/2-s are too long at N<50; a kink at N =50,
... nice agreement with the RIKEN N>50 data

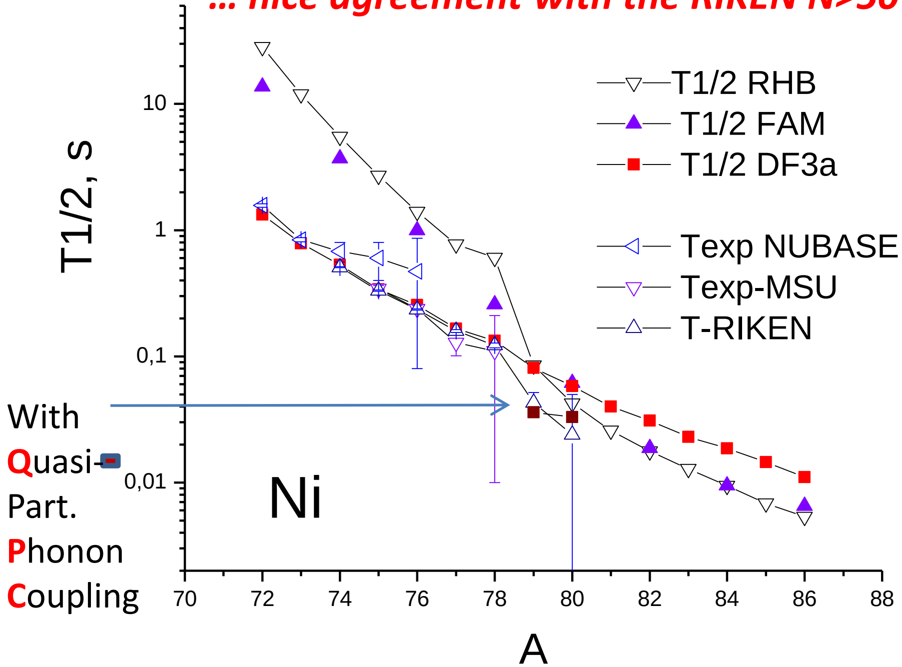

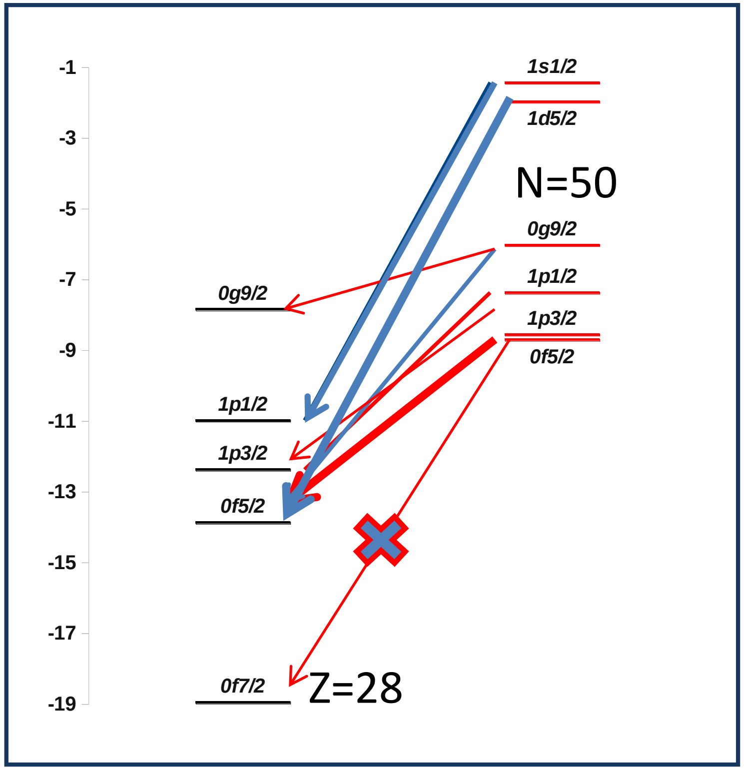

Balance of the GT and FF strengths !

$$\%FF = \lambda_{FF} / \lambda$$

DF3 predicts:
%GT > %FF at N<50 , moderate %FF at N>50

N≤ 50
Main GT
n0f5/2 → p1f 5/2
vs.
Unique FF
(rank 2, Δ J=2)
n0g9/2 → p1f 5/2

N > 50
Non-unique FF
(rank1, Δ J=0,1)
n1d5/2 → p0f 5/2...

N ~ 50 REGION: *% FF or GT should reflect the selection rules*

*RHB : **higher FF strength in Qb-window .***

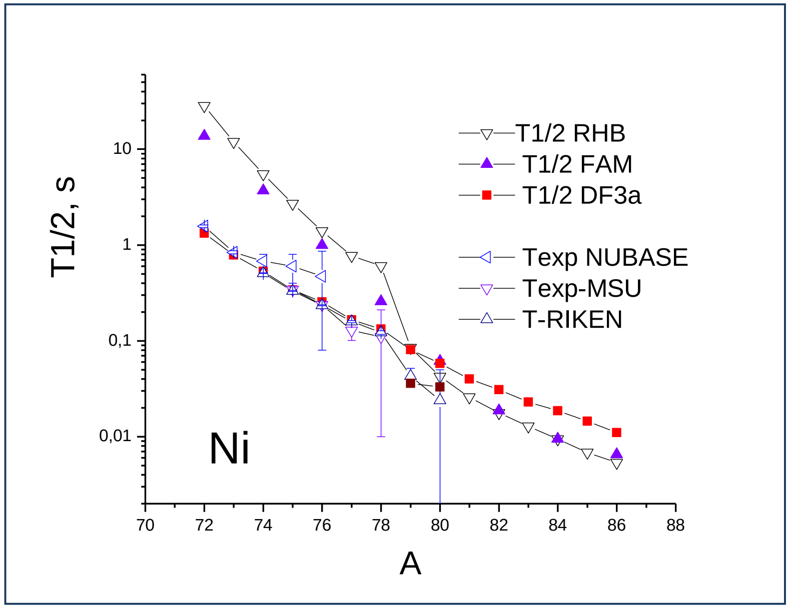

%FF = λ_{FF}/λ = [t(GT) – T(GT+FF)] / t(GT)

At A<78: ***Only Unique FF contribute.***
*(1g9/2→0f 5/2), rank 2, **Δ J= 2***

At A>78: ***Non-unique FF also appear***
*(2d5/2, 2s 1/2→2p1/2,3/2, 1f5/2), rank 1, **Δ J= 0,1***

NB! Unique FF are suppressed by factor $\xi = Ze^2/2R\, m_e c^2$
For Z=28 $\xi \le 10$

RHB at N < 50: % FF is 20 - 40%

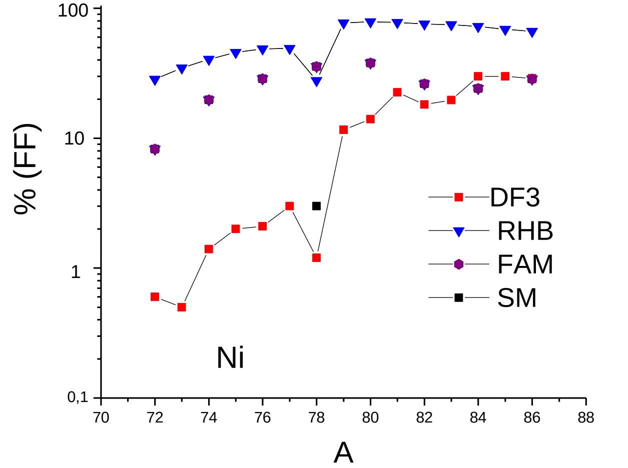

RHB, FAM :

At A<78: *U-FF amount of 30-50% and **T1/2 are longer**.*

At A>78 *%FF ~70-80% : **T1/2 are OK !***

DF3

At A<78: *U-FF contribution is ≤ 3%*

At A>78 *%FF ~30%.*

In compliance with the expected suppression factor ξ

T1/2 are OK for A≤ 80 !

N ~ 50 REGION. *Different functionals: different Sxn, Q_β, Eqp and* ***Pxn***

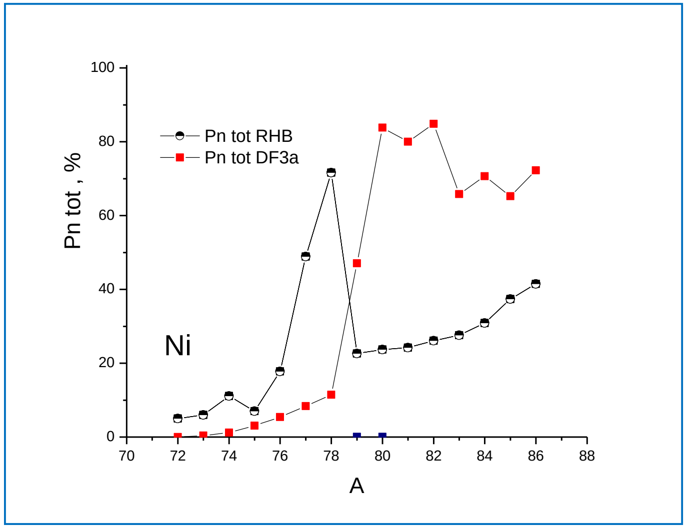

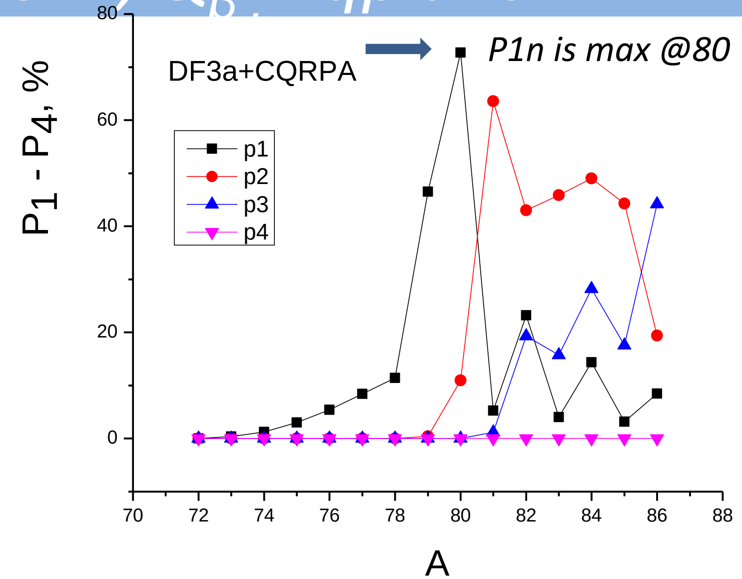

DF3 : P1n grows up to A=80 due to higher %GT and decreases at A>80 due to increasing %FF. At A>81 P2n is getting stronger than P1n

At A=86 P3n > P2n - exactly like in DF3.

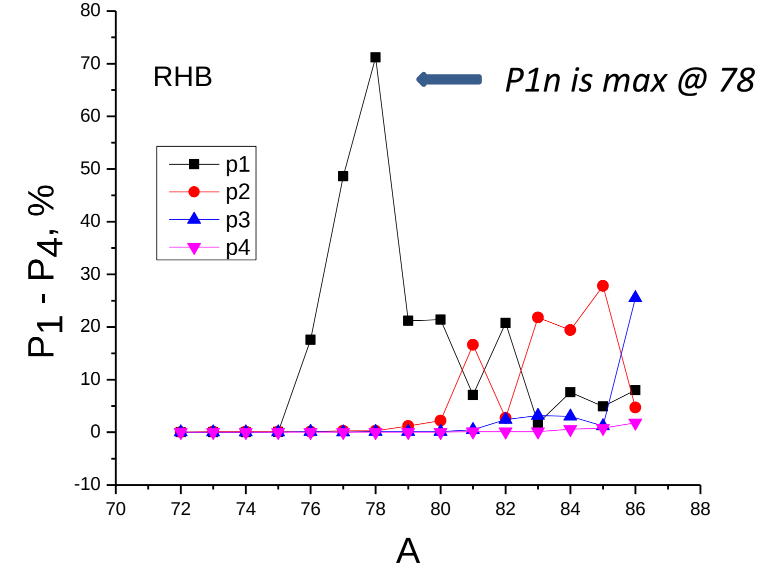

RHB : P1n grows at A<78 , drops at A=78+1n . At A>81 oscillation of P1n and P2n .

RHB : max P2n at A=85 : ~28%
DF3: max P2n at A=81 : ~65%
In DF3: P2n is nearly 2.5 times higher

Different $S_{JLS}(w)$.

N ~ 82 REGION. RIKEN-2014

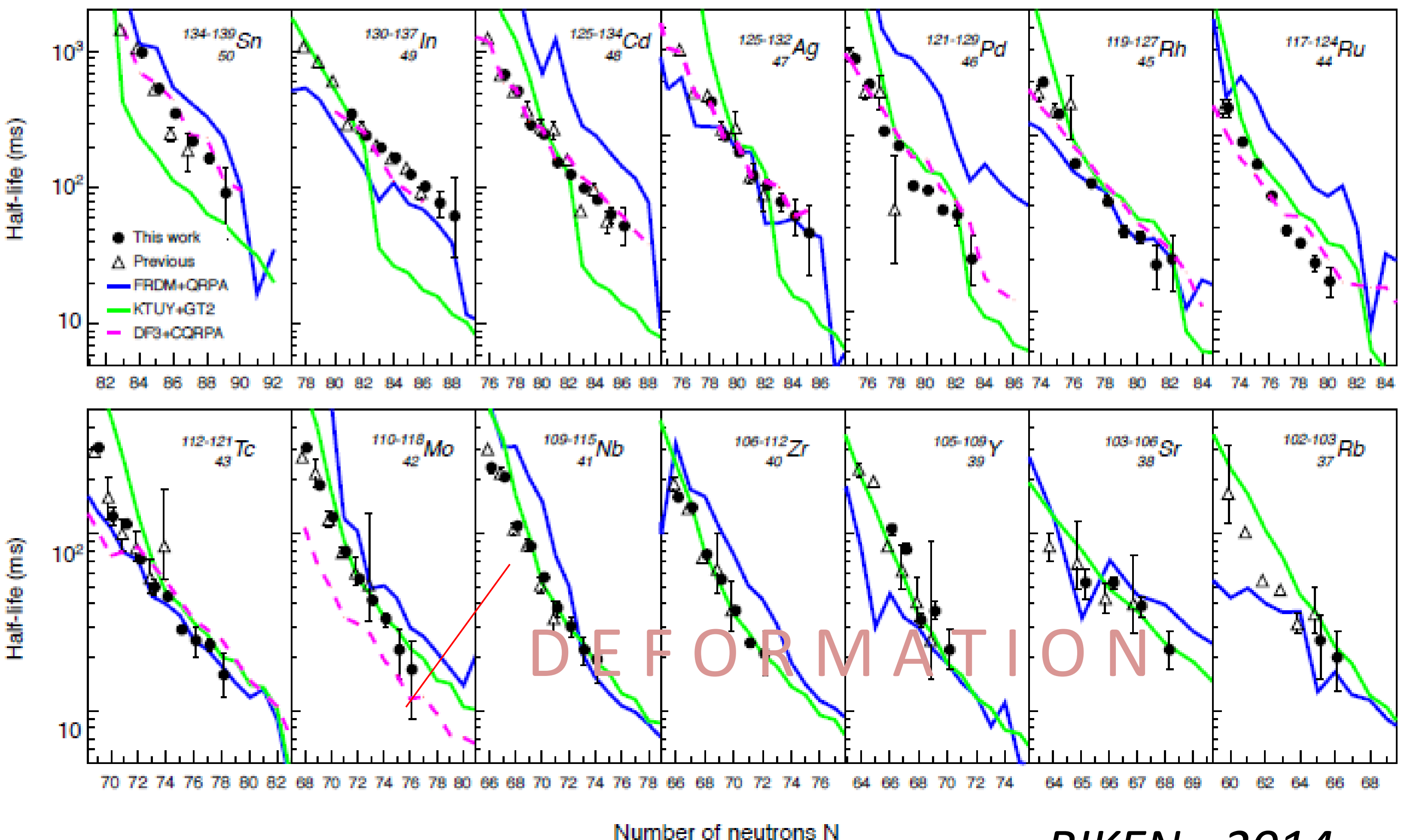

RIKEN - 2014

DF+CQRPA - closer to data - shorter than FRDM.
An impact on the r-process timescale.

G. Lorusso et.al.
Phys.Rev. Lett. 114, 192501 (2015)

N ~ 82 REGION : 132Sn and beyond

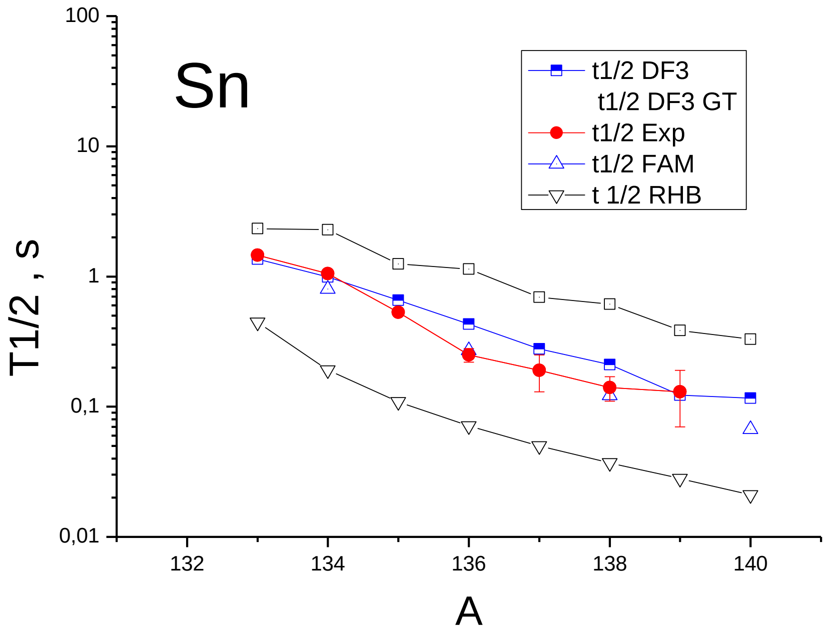

132 Sn	*T1/2, s*	*%FF*
Exp.	*39.7*	-
DF3a	*35.7 s*	*2.7%*

132 Sn	*T1/2, s*	*%FF*
RHB	***610 s***	*74%*
FAM	***820 s***	*70%*

132 Sn data half-lives are overestimated up to the factor of 20 by RHB and FAM.

The reason can well be in high %FF !

At 132Sn GT dominate, for N>82 %FF grows with N, for N>86 % GT wins

For 132Sn %FF in DF3 is consistent with exp. decay scheme.

$$\%FF = \lambda_{FF} / \lambda = [t(GT) - T(GT+FF)] / t(GT)$$

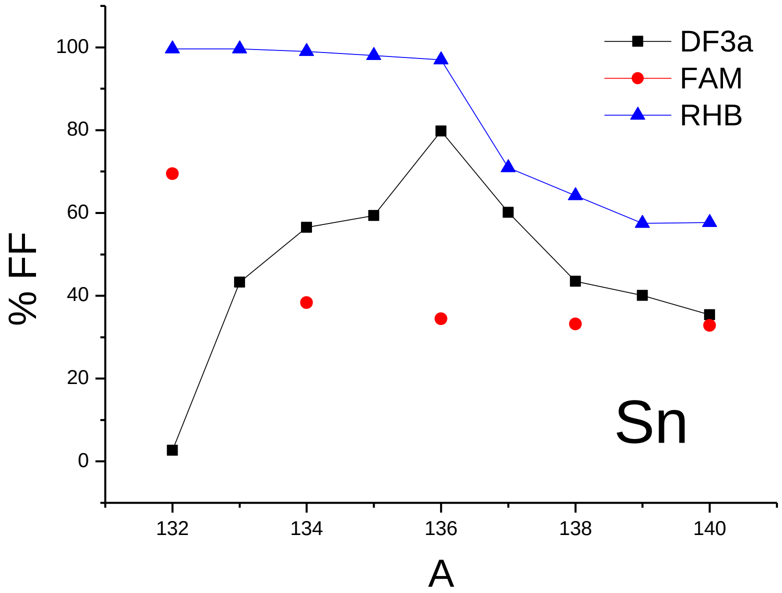

99% branching - 1⁺ (1.325MeV)
0.17% for 2nd to 4th FF decays

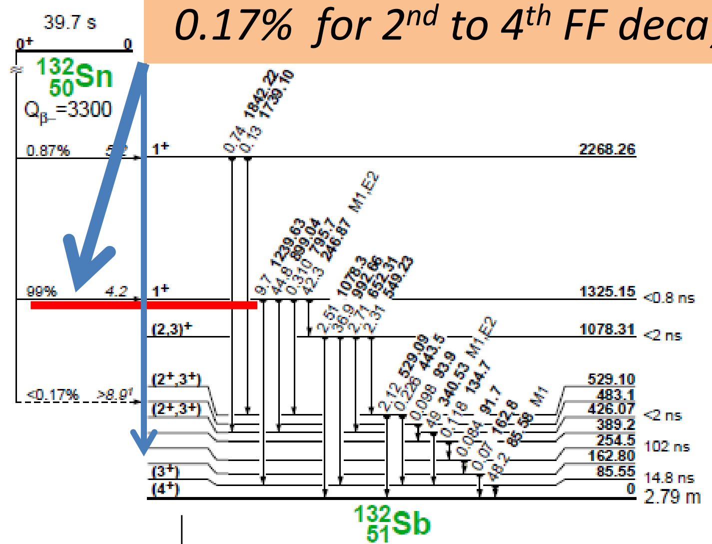

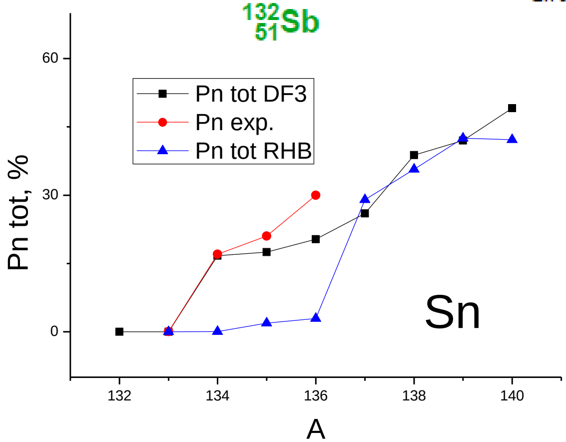

For 40<Z<50 RHB predicts reasonable behavior of %FF.
Z=50 - semi-magic Sn isotopes …

Pn (A) DF3 and RHB are consistent with "their" %FF

N = 50 and N=82 ISOTONES.

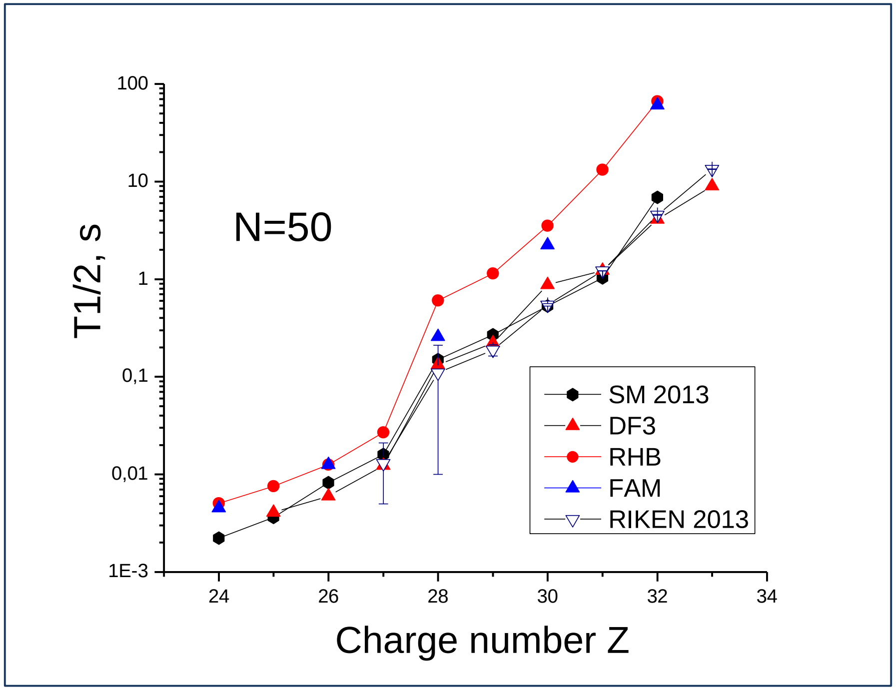

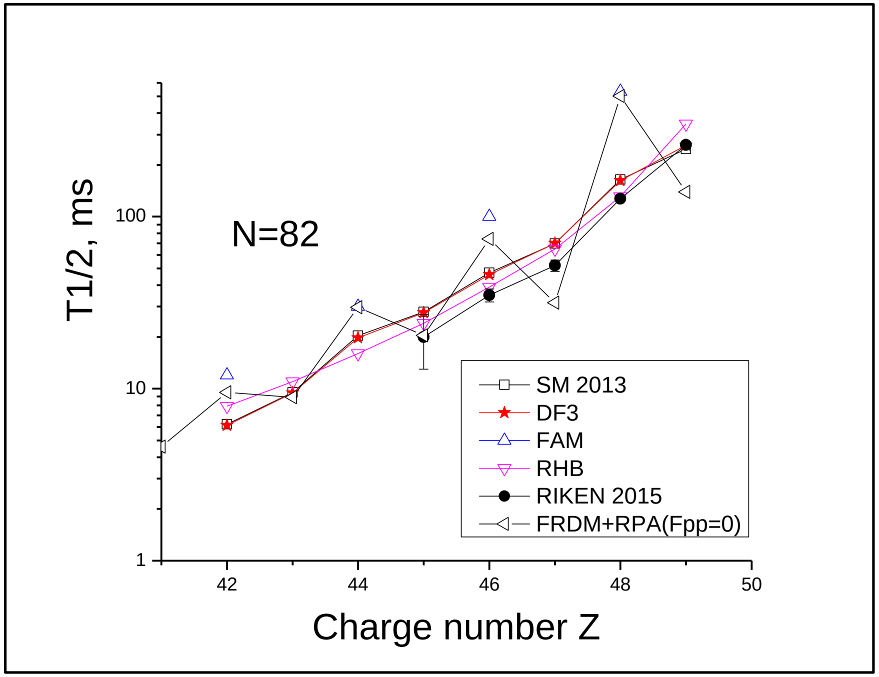

- ***T1/2(N=50): overestimated by RHB and FAM***

- ***T1/2(N=82): overestimated by FAM***
- ***SM, RHB and DF3 are close to each other***
- ***FRDM+RPA: odd-even staggering is due to F_{pp}=0***

N ~ 82 REGION:
^{134}Sb : an impact of FF decays
^{140}Sb : g.s. spin inversion effect as in $^{84-85}$Ga

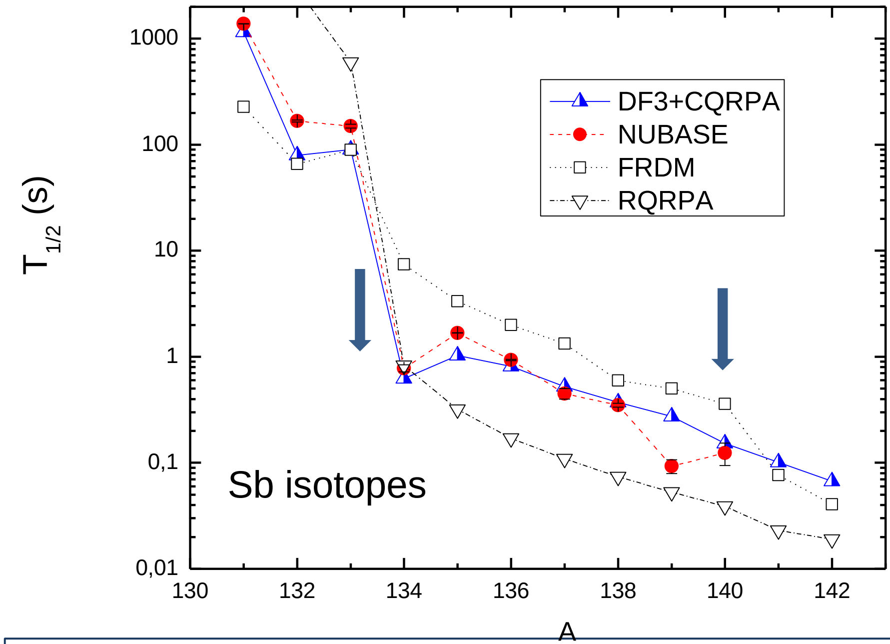

1. Very strong reduction of the T1/2 at A=134 (N=82+1n) is due to the opening of the g.s 0⁻ → g.s. 0⁻ FF decay

Stabilization of the half-lives at A=140. The Exp. gives an INCREASE of T1/2

T1/2 exp (^{139}Sb)=93 (+14 -3) ms

T1/2 exp (^{140}Sb)=124 (30) ms

Also has been seen in 84-85Ga M. Madurga, …. I.N.B. … et al. Phys. Rev. Lett. 110, 117 (2012)

2. EURICA : N. Lozeva et al., Phys.Rev. 93, 014316 (2016)
7/2+ → 5/2+ g.s. spin inversion at N =89

*DF approach: A provision to fix the **J / π of the odd nucleon** before variation.*
Gives correct g.s. spin-parity and describes possible g.s. spin inversion.

N ~ 82 REGION: ^{136}Sb : FF decay impact on Pn tot.
Importance of QPC – redistribution of the strength near Sxn.

Z>50, N>82

Strong suppression of Pn tot due to the FF decays undergoing outside the Qbn- windows

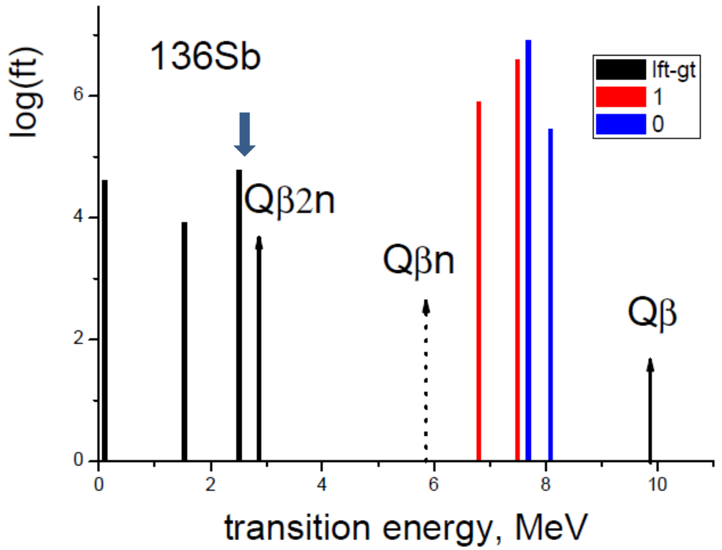

Pn(Df3) = 5.4% , P2n= 3.1 %

Pn(RHB)=3.8%, P2n= 0.2%

Pn exp= 16.3(0.32)%,
P2n=0.26(2) – 2.0(0.2)

Resulting P_{xn} - values are extremely sensitive to the strength function near the xn-thresholds !

IMPORTANCE OF Quasiparticle-Phonon Coupling !

DF3 with np-nh spreading

Pn (Df3-s) = 15.6% , P2n= 0.7 %

Skyrme-FRSA + Quasiparticle-Phonon Coupling

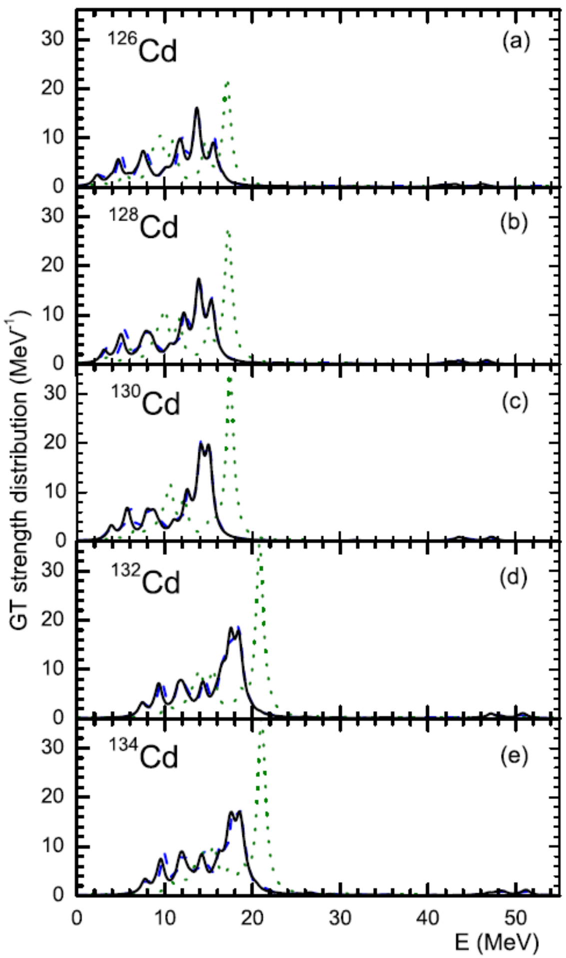

FIG. 3. GT strength distributions of $^{126-134}$Cd as functions of the excitation energy of the daughter nuclei. The QRPA calculations with the tensor interaction and without the tensor interaction are shown as dashed lines and dotted lines, respectively. The solid lines correspond to the quadrupole-phonon coupling effect on the QRPA results obtained with the tensor interaction.

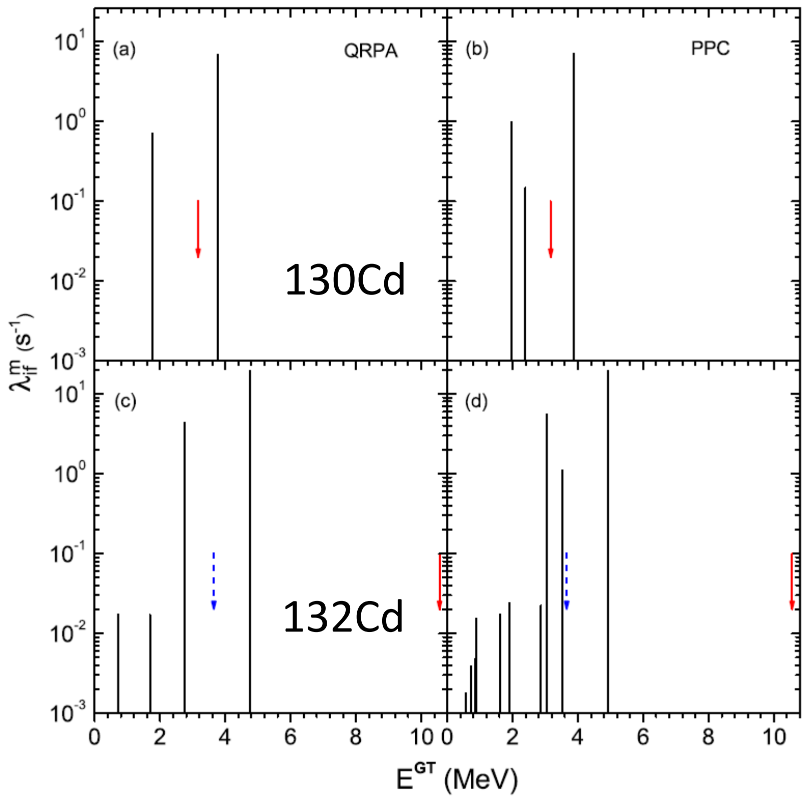

FIG. 6. The phonon-phonon coupling effect on the β-transition rates in ^{130}Cd (top) and ^{132}Cd (bottom). The left and right panels correspond to the calculations within the QRPA and taking into account the $[1_i^+ \otimes 2_{i'}^+]_{QRPA}$ configurations, respectively. The calculated $Q_{\beta 1n}$ and $Q_{\beta 2n}$ energies are denoted by the solid and dashed arrows, respectively.

PHYSICAL REVIEW C 95, 034314 (2017)

Multi-neutron emission of Cd isotopes

A. P. Severyukhin,[1,2] N. N. Arsenyev,[1] I. N. Borzov,[3,1] and E. O. Sushenok[1,2]

Skyrme-FRSA + QPC.
Beta-rates with tensor and pp- interactions incl.

(w/o pp)

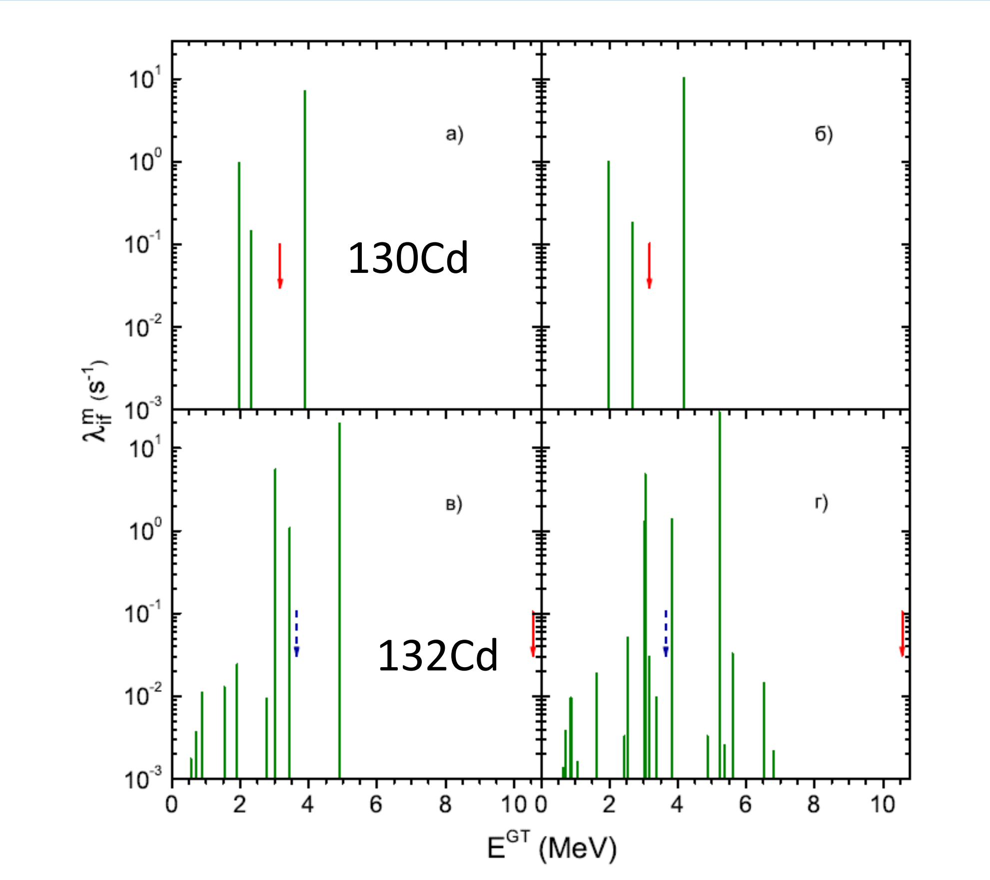

(with pp)

Sushenok E.O., Arseryev N.N., Severyukhin A.P., Borzov I.N.,
Preprint JINR P4-2017-40

N~126 region. Predictions for the GSI experiments 2014-16

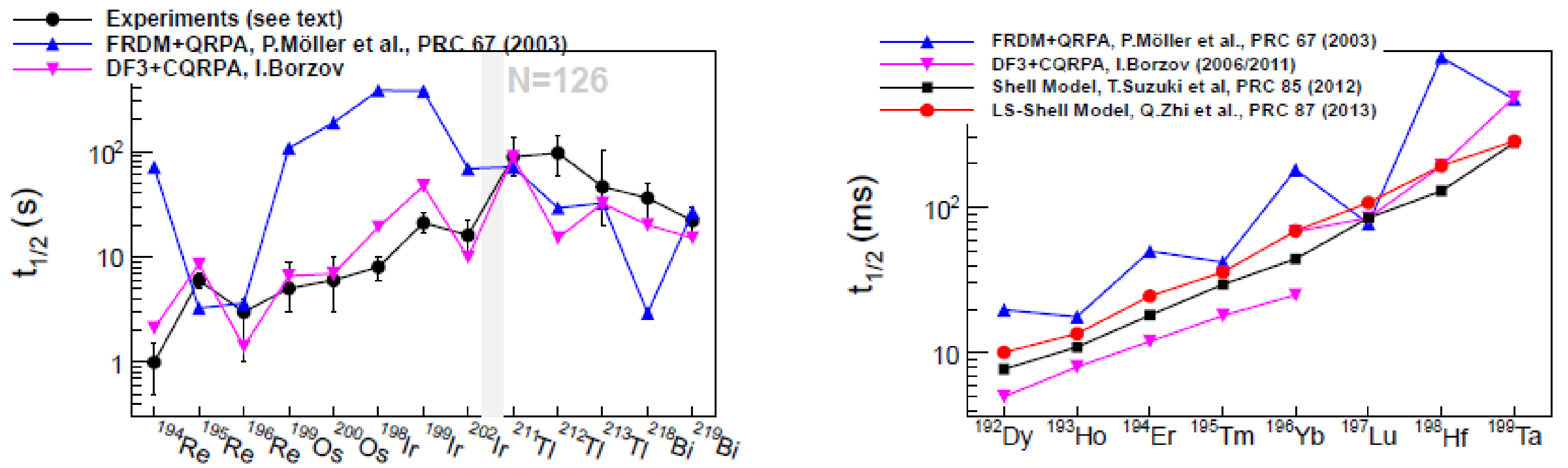

Figure 2. (Left) Comparison between theoretical predictions and measurements in the region around $N = 126$. Experimental values from ^{194}Re to ^{202}Ir are from Ref. [8], values between ^{211}Tl and ^{219}Bi are from Ref. [11]. (Right) Theoretical values published in the literature for the waiting point nuclei along $N = 126$ (adapted from Ref.[17]).

Beyond N = 126. GSI, Darmstadt.

T1/2 for 20 new isotopes of Au to Bi . Pn for Hg and Tl.

First measurement of several β-delayed neutron emitting isotopes beyond N=126

R. Caballero-Folch[1,2], C. Domingo-Pardo[3,*], J. Agramunt[3], A. Algora[3,4], F. Ameil[5], A. Arcones[5], Y. Ayyad[6], J. Benlliure[6], I.N. Borzov[7,8], M. Bowry[9], F. Calviño[1], D. Cano-Ott[10], G. Cortés[1], T. Davinson[11], I. Dillmann[2,5,12], A. Estrade[5,13], A. Evdokimov[5,12], T. Faestermann[14], F. Farinon[5], D. Galaviz[15], A.R. García[10], H. Geissel[5,12], W. Gelletly[9], R. Gernhäuser[14], M.B. Gómez-Hornillos[1], C. Guerrero[16,17], M. Heil[5], C. Hinke[14], R. Knöbel[5], I. Kojouharov[5], J. Kurcewicz[5], N. Kurz[5], Yu. A. Litvinov[5], L. Maier[14], J. Marganiec[18], T. Marketin[19], M. Marta[5,12], T. Martínez[10], G. Martínez-Pinedo[5], F. Montes[20,21], I. Mukha[5], D.R. Napoli[22], C. Nociforo[5], C. Paradela[6], S. Pietri[5], Zs. Podolyák[9], A. Prochazka[5], S. Rice[9], A. Riego[1], B. Rubio[3], H. Schaffner[5], Ch. Scheidenberger[5,12], K. Smith[5,20,21,23,24], E. Sokol[25], K. Steiger[14], B. Sun[5], J.L. Taín[3], M. Takechi[5], D. Testov[25,26], H. Weick[5], E. Wilson[9], J.S. Winfield[5], R. Wood[9], P. Woods[11] and A. Yeremin[25]

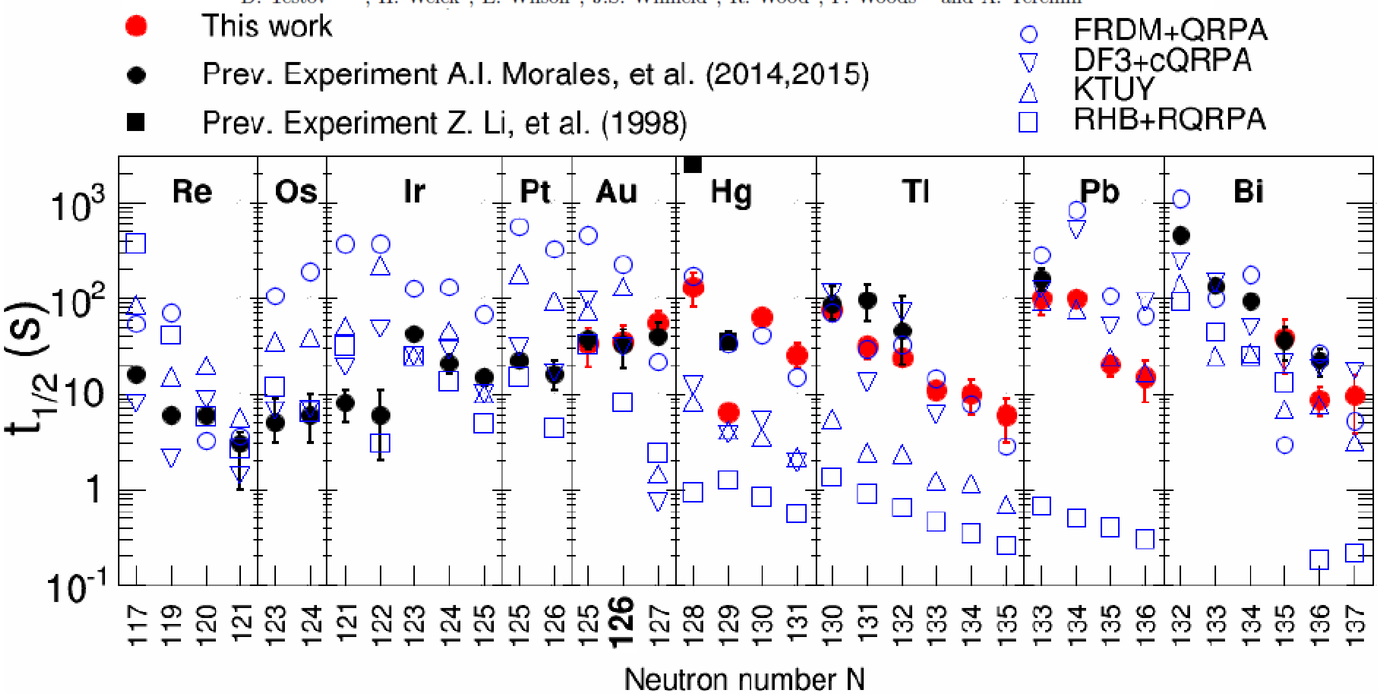

FIG. 3. Experimental half-life values (solid symbols) on both sides of $N = 126$ from previous experiments [48–50] (bold circles) and [51] (bold squares) and from the present work (red circles). Open circles show published theoretical half-lives [22, 23, 25, 32, 52] (see legend).

Physical Review Letters 117, 012501 (2016)

N ~ 126 REGION / Low Q_β decays.

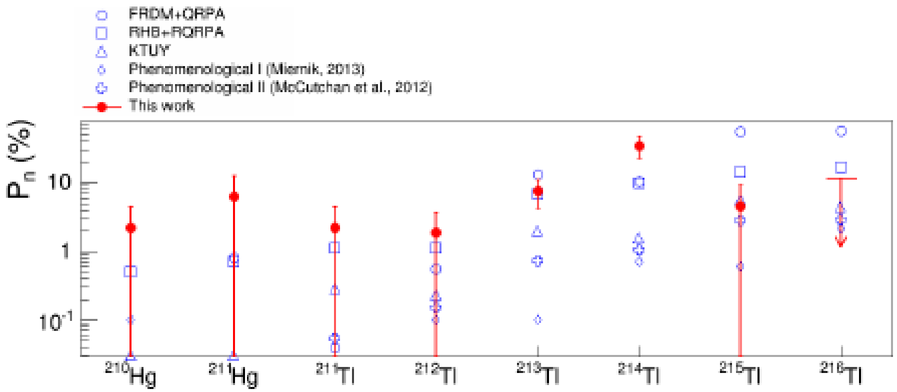

FIG. 4. Measured neutron emission probability (%) or upper limit (^{216}Tl) for the Hg- and Tl-isotopes (solid red circles and arrows). Theoretical predictions from Refs. [22, 25] and phenomenological models [30, 31] are shown with open symbols.

Physical Review Letters 117, 012501 (2016)

Additional constraints when comparing microscopic models with experiment can be found in the neutron-branching ratios of the Tl-isotopes, which are shown in Fig. 4. The discrepancies found between the RHB+RQRPA predictions and the measured Tl-decay half-lives (Fig. 3) are at variance with the quite good agreement that is found with the measured neutron branching ratios. As the GT and FF decays are treated in a single RQRPA framework, this may reflect that the integral of GT+FF strength is overestimated both in $Q_{\beta n}$ and Q_β windows. The good agreement between the experimental half-lives and the FRDM+QRPA predictions for the entire Tl-isotopic chain (Fig. 3) is in contrast with the factor of five discrepancy found for the FRDM+QRPA predicted branching ratios of ^{215,216}Tl.

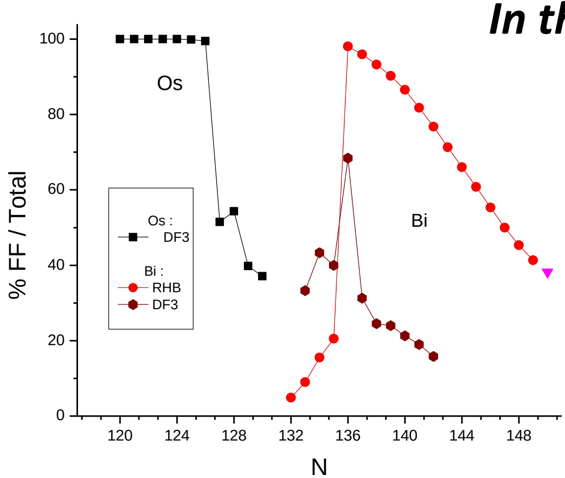

In the Os chain (N-Z→ 52), %FF(A) is similar in RHF and DF3

In the Bi chain, %FF (A) at high N-Z→ 64 are different

As in all considered isotopic chains, %FF (A) is important for simultaneous description of the T1/2-s and Pn-s

Model
Shell-model [1]
DF+CQRPA [2]
RHB+QRPA [3]
FAM [4]
FRSA [5]

CONCLUSIONS

Comparison of the RF3, RHB and FAM:

Some difference in describing the "standards".

Main reasons:

Density functional structure;

Imposed constraints (β_2, s.p. basis, fitting protocol…)

Structural indicators:

ε_{sp}, Q_β, S_{xn} and $T_{1/2}$, Pn tot, Pxn

should be treated simultaneously

Sensitive marker: % of the GT and FF in the total rate

Competition of the Gamow-Teller and first-forbidden (FF) decays.

Consistency with decay schemes.

1. Q. Zhi, E. Caurier, J. Cuenca-Garc'ia, K. Langanke, G. Mart'inezPinedo, K. Sieja, Phys. Rev. **C87** (2013).
2. I.N. Borzov., Phys. Rev. **C67**, 025802 (2003).
3. T. Marketin, L.Huther, G. Martinez-Pinedo, Phys. Rev. **C 93**, 025805 (2016).
4. M. T. Mustonen, T. Shafer, Z. Zenginerler, J. Engel., Phys.Rev. **C90**, 024308 (2014);
   M. T. Mustonen, J. Engel., Phys.Rev. **C93**, 014304 (2015).
5. A.P. Severukhin, V.V.Voronov, I.N. Borzov, N.N.Arsenyev, N.Van Giai., Phys. Rev. **C90** 044320 (2014).
   A. P. Severyukhin, N. N. Arsenyev, I. N. Borzov, and E. O. Sushenok., Phys. Rev. **C95**, 034314 (2017).

(III) Sensitivity of the r-process to nuclear input : beta-decay rates

A. Impact of new experimental data on r-process abundancies.

B. Microscopic models performance vs "standard FRDM"

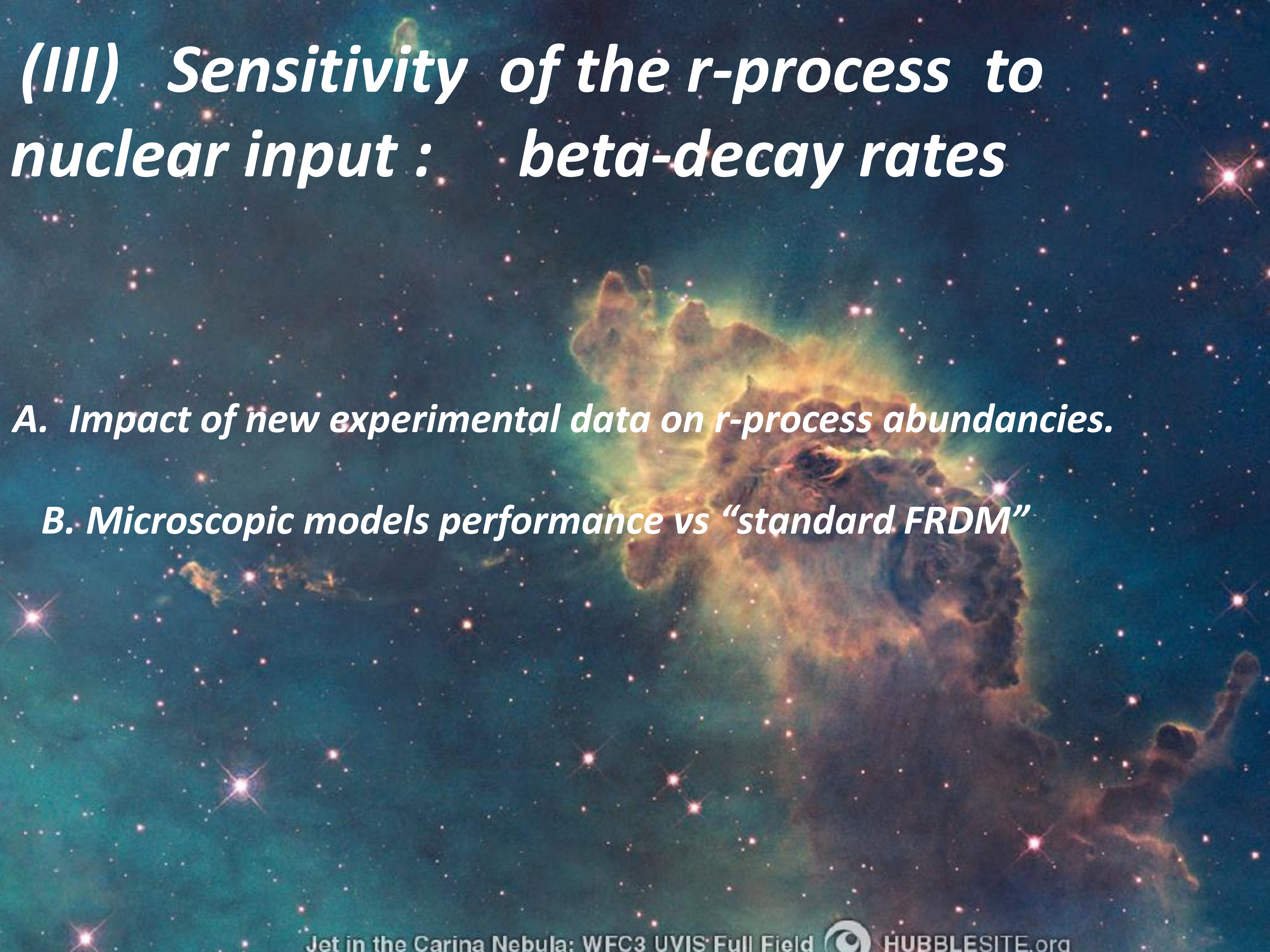

Classical model can not solve the problems of the r-process site and mechanism.

Few "state of art" astrophysical scenarios

1. ***Supernovae "neutrino-driven wind" or PNSW.***
   a) "HOT" r-process;
   b) "COLD" r-process . (No (n,ϒ) - (ϒ,n) equilibrium)
   S. Wanajo Ap.J.Lett. 770 L22 (2013)
2. ***Neutron star merger***
   "COLD" r-process . (Y n / Y seed > 1 , fission cycling is possible)
   S. Rosswog et al. MNRA Soc. 439, 744 (2014)
3. ***Magneto-rotational supernovae***
   Prompt-magnetic jets
   C. Winteler et al. Ap. J.lett 750, L22 (2012)
4. ***Quark-hadron phase transition.***
   N. Nishimura et al. Ap.J 758, 9 (2012

(Nn, T , Ye or initial composition, S/b, Nn/Nseed)

Sensitivity of the r-process abundances to beta-decay rates

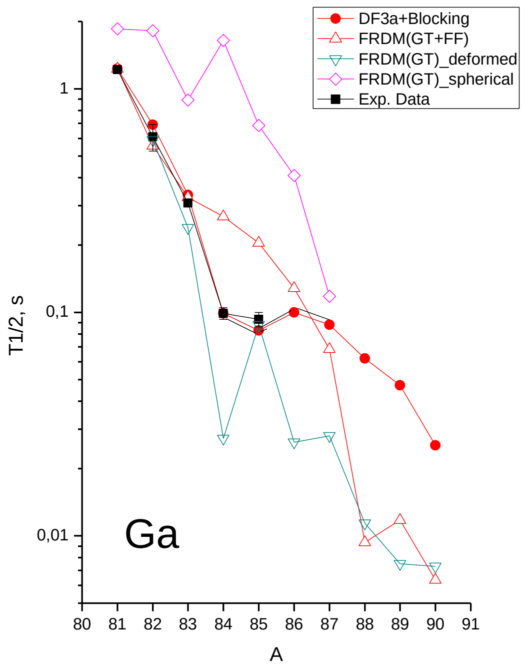

M. Madurga, R. Surman et. al. PRL 109 (2012

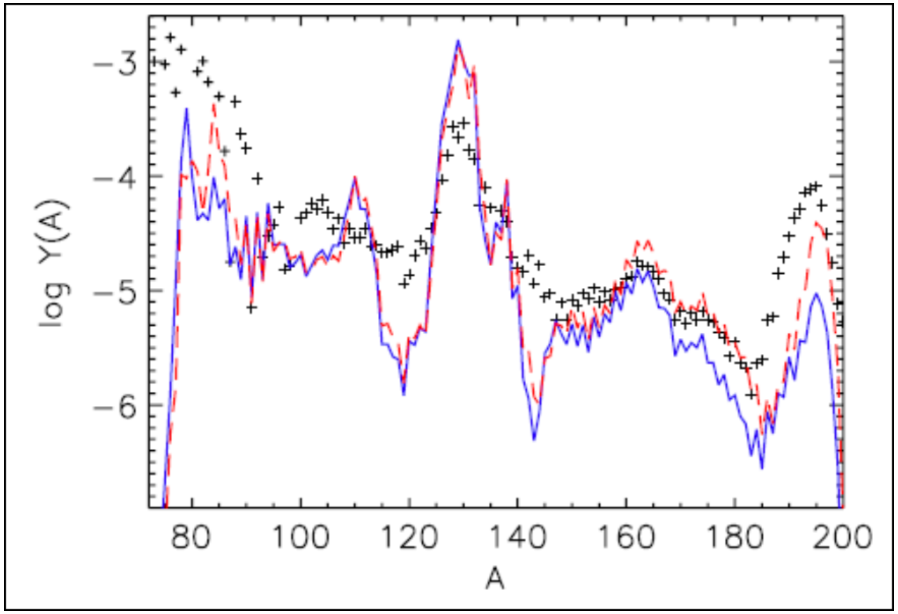

Fig. 1. (left) The r-process abundances (note logarithmic scale) calculated using new experimental and theoretical half-lives (red curve) are compared to previous FRDM simulations (blue curve).

Standard FRDM-RPA+Gr.Th (GT+FF):

- ***overestimates exp.data at N<54***
- ***and shorter than DF3 at N>54 (A=85)***

The longer DF3 half-lives above A=85 *caused more material trapped in the first peak. Since less material escape the A=80 region , fewer neutrons are used up, more neutrons available for capture in A>90 region. The path is a bit further from stability, where the half-lives are faster, less material trapped in A=130 peak. These two effects combine to greatly increase the abundances at A>140. Substituting the FRDM half-lives for A=27-32,51 leads to even more significant redistribution of the pattern including more vigorous third peak. New half-lives allow the r-process to reach higher mass before freeze out efficiently enhancing the abundancies at A>140.*

Log(T_DF3/T_FRDM)

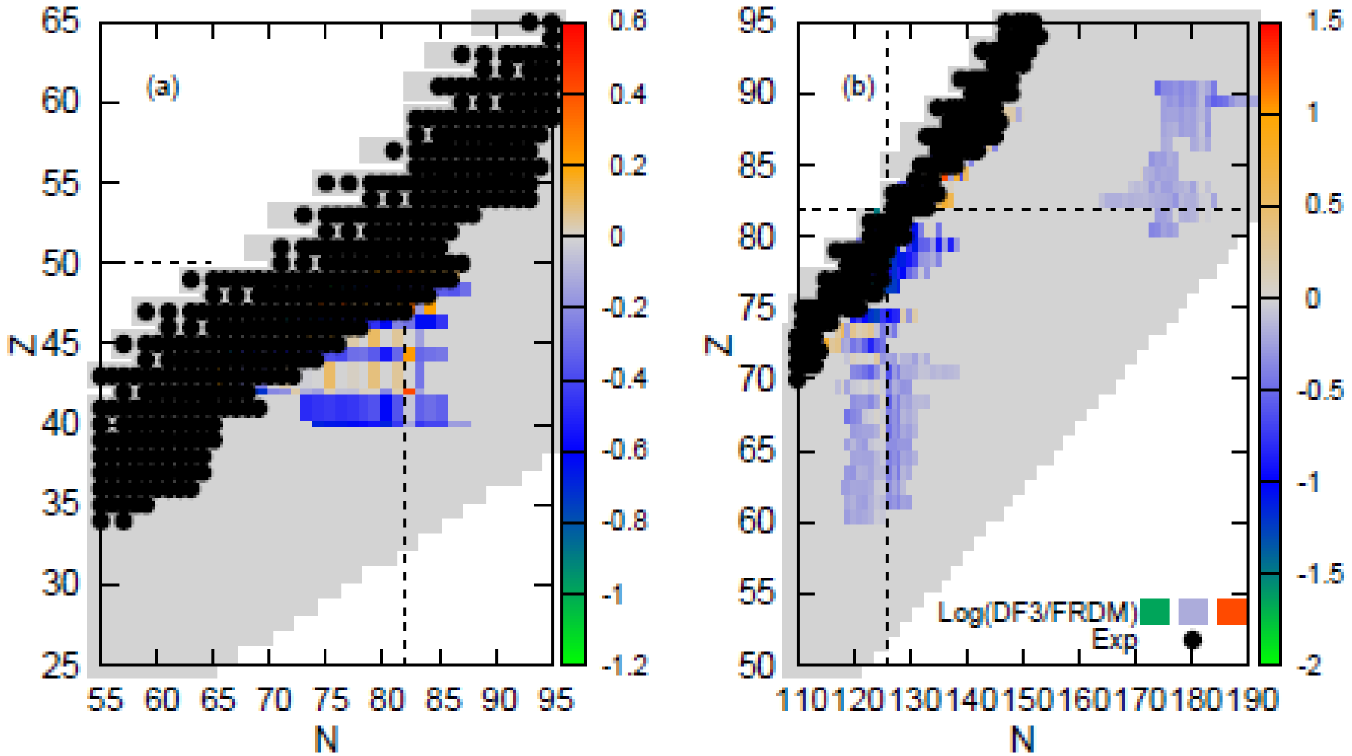

FIG. 1: Logarithm of the ratio of the two sets of β decay rates used in our nucleosynthesis calculations. The black points mark the nuclei with experimental half lives. The dashed lines correspond to magic numbers.

Local and global effects of beta decays on r-process

O. L. Caballero,[1,2,3] A. Arcones,[2,4] I. N. Borzov,[5] K. Langanke,[4,2,6] and G. Martinez-Pinedo[2,4]
[1] *ExtreMe Matter Institute EMMI, GSI Helmholtzzentrum für Schwerionenforschung GmbH, 64291 Darmstadt, Germany*
[2] *Institut für Kernphysik, Technische Universität Darmstadt, 64289 Darmstadt, Germany*
[3] *Department of Physics, University of Guelph, Guelph, Ontario N1G 2W1, Canada*
[4] *GSI Helmholtzzentrum für Schwerionenforschung, Planckstr. 1, 64291 Darmstadt, Germany*
[5] *Joint Institute for Nuclear Research, 141980 Dubna, Russia*
[6] *Frankfurt Institute for Advanced Studies, 64289 Frankfurt, Germany*
(Dated: April 29, 2014)

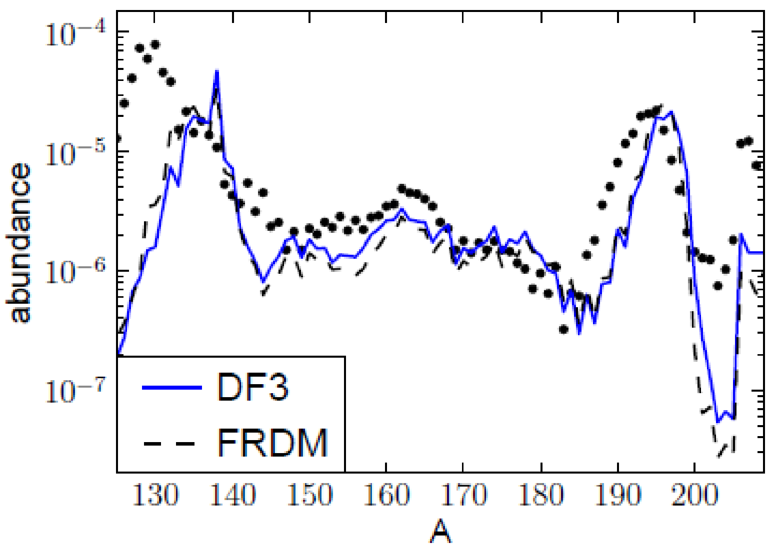

FIG. 2: Final abundances for cold r-process conditions based on two sets of beta decay rates (see text for details). The dots represent the scale solar abundances.

Our two beta decay sets differ mainly for nuclei in the regions of the magic neutron numbers $N = 82$ and $N = 126$. Therefore, one expects abundance differences between our two r-process simulations in the region of the second and third peak, i.e., $A \approx 130$ and $A \approx 195$, peaks. We can hence conclude that the changes in the beta decay rates have two effects on the r-process abundances: a local which affects the abundances in the region of nuclei with changed half-lives and a global that changes the general abundances pattern, including nuclei which half lives have not been modified. Global changes occur because changes in the nuclear half lives influence the flow of matter to heavier nuclei. Furthermore, such changes affect how fast neutrons are exhausted during the r-process with the important consequence that the freeze-out can occur under different astrophysical conditions. This can have important impact on the final r-process abundances.

arXiv:1405.0210 (2014)

110 Beta decay half-lives of very neutrom-rich Rb to Sn. G. Lorusso et al. Phys.Rev. Lett. 114, 192501 (2015). 40 new half-lives.

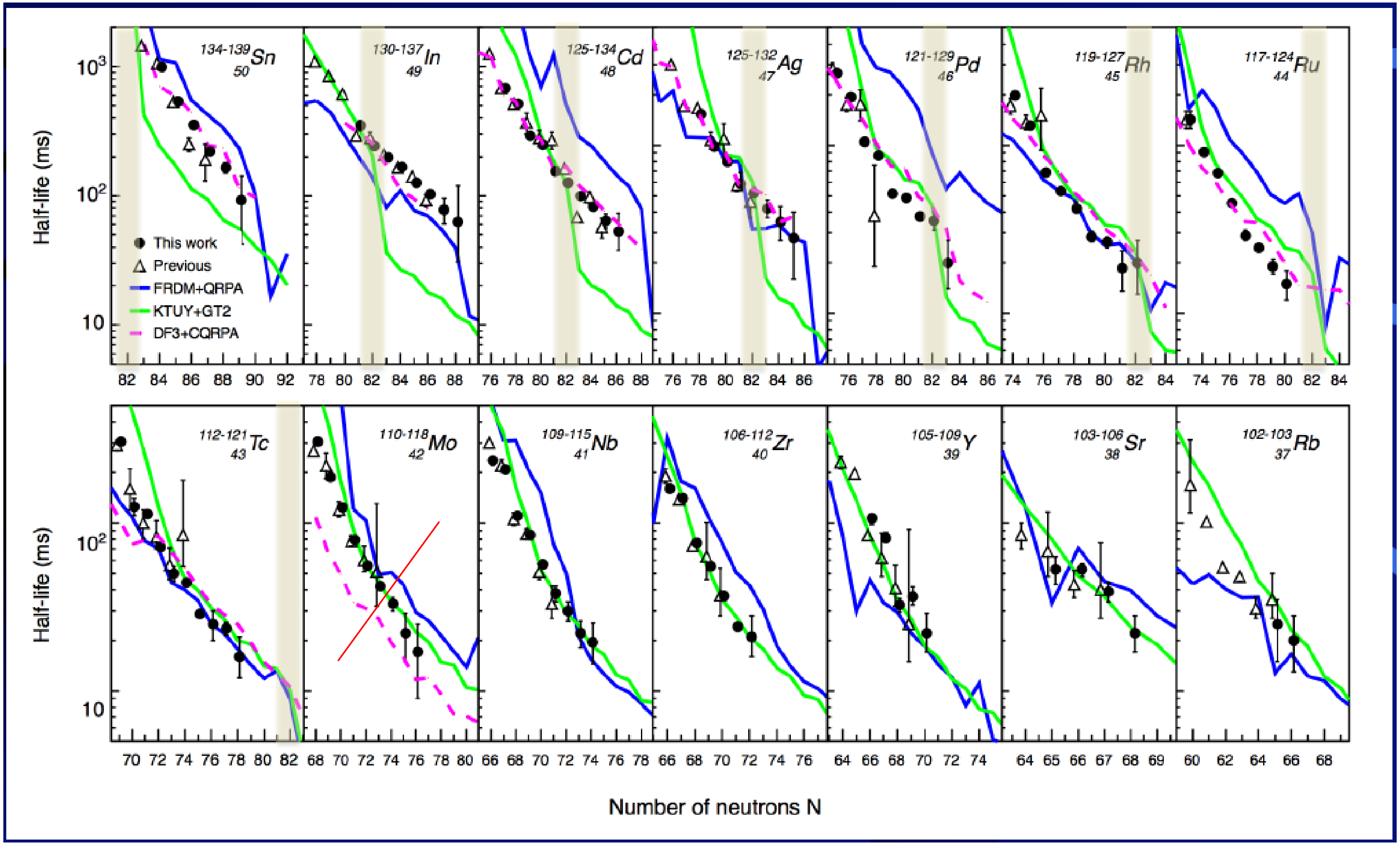

DF3+CQRPA is closer to exp. for ***spherical nuclei (Z>42)*** *cf. FRDM and GT2*

Using 110 new half-lives from RIKEN

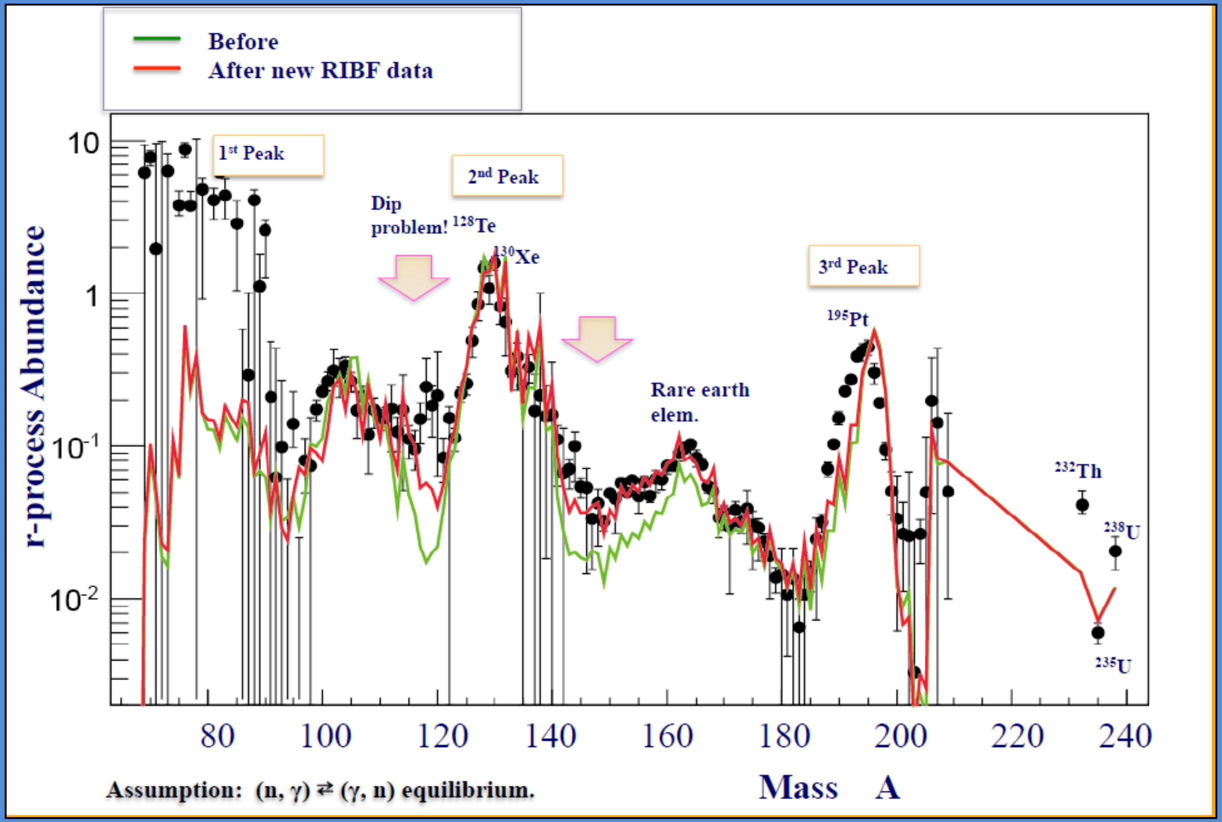

Local and Global impact of new half-lives:

1. Soften under-production @ A=130.
No shell quenching needed.
Still a "dip" problem @ A=120.

2. Using new half-lives of Ag, Cd,In and Sn(N>82) help to IMPROVE description of the REE Peak @ A=160 !

Key to the universality of the r-process: REE Peak Z>55, A~160 in SoS and MPS

Abundancies of Rear-Earth Elements match coherently both in SoS and (OLD)Metal-Poor Stars!

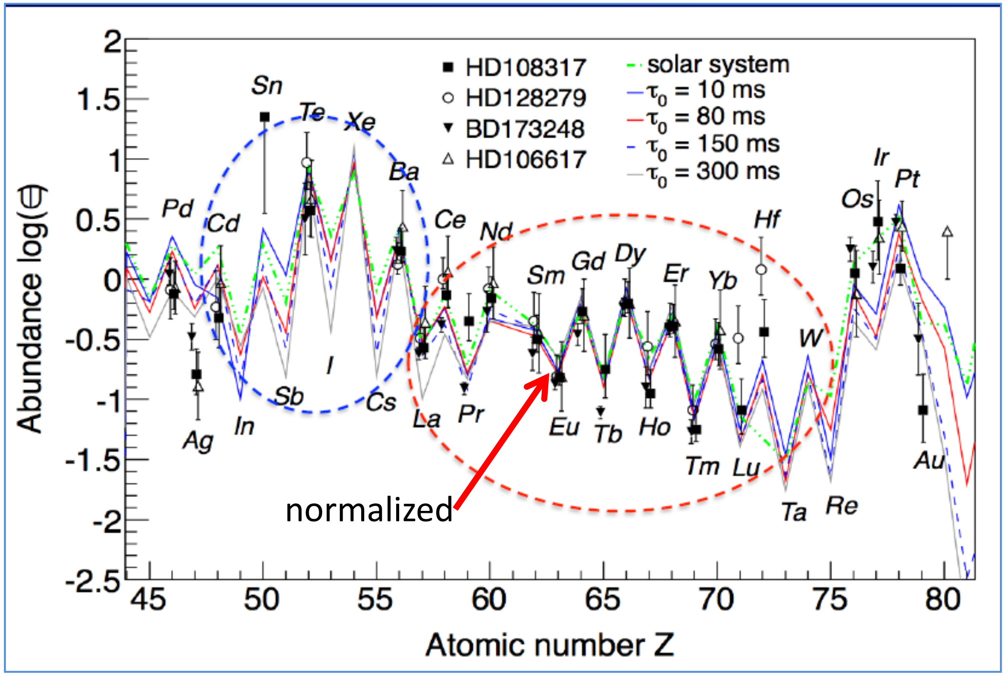

Comparison of elemental r-process abundancies in 4 metal-poor stars (MPS) and in solar system (SoS) with calculated for a wide r-process parameter space given by the expansion time ***τ_0=10 -300ms.*** ***Normalized to the abundance of Eu.***

In SoS – the abundance pattern is a result of many r-process events averaged over τ .
In contrast, earlier generation of stars (MPS) display very few r-process events !

Example: in MPS robust Te production is known. It is supported by above calculation for τ_0=10 -300ms. Despite the different r-process conditions varying the outputs for 4 stable Te isotopes , the compensation occurs resulting in robust Te production (cf. with I and Cs having one stable isotope and being very sensitive to the r-process conditions).

EURICA 94 β-Decay Half-Lives of Neutron-Rich 55Cs to 67Ho.

J.Wu et.al. Phys. Rev. C 94, 064322 (2016).

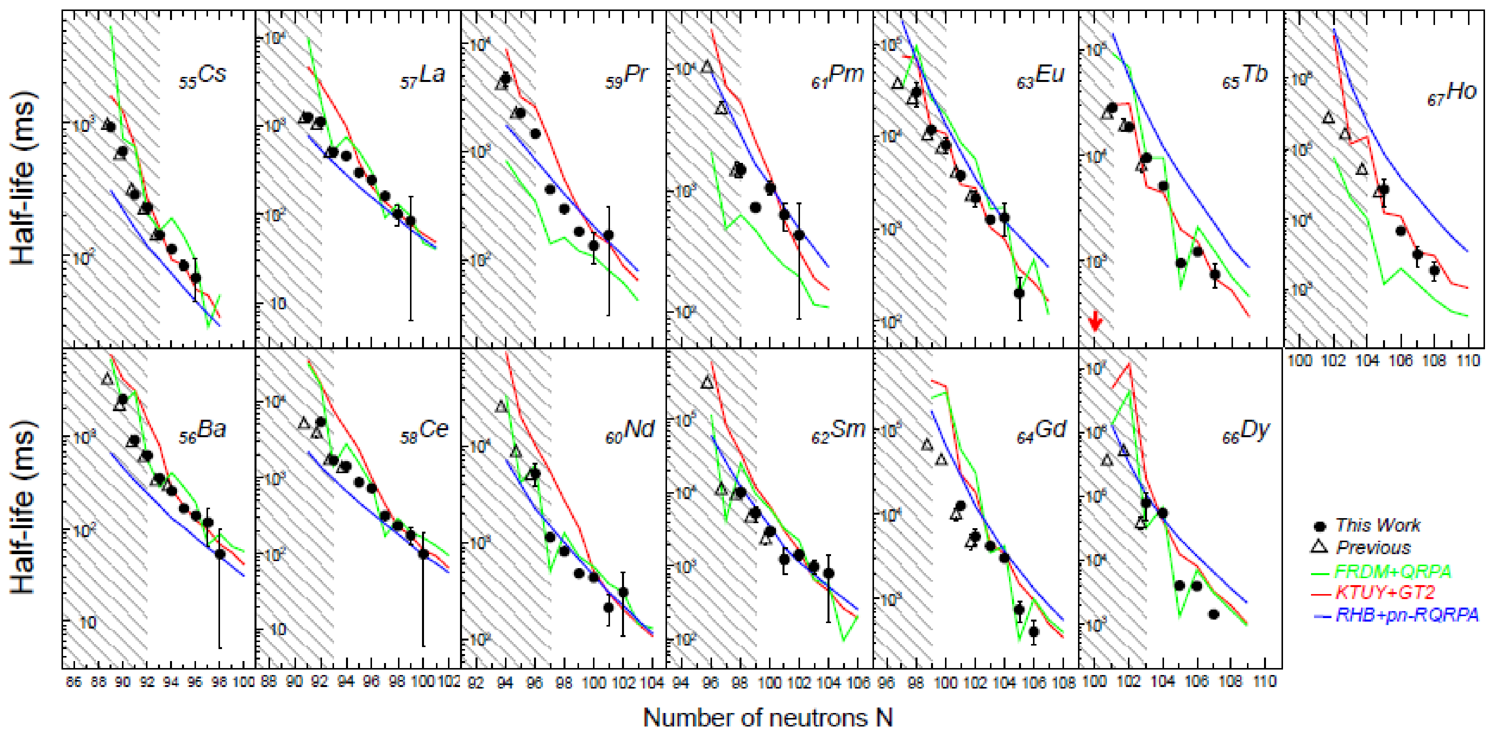

FIG. 3. (color online). Systematic trends of β-decay half-lives from this work (solid circles) and previous measurements (open triangles) [26] with neutron number for thirteen elements. The measurements are compared to predictions of three theoretical models: FRDM+QRPA [28] (green), KTUY+GT2 [29, 30] (red), and RHB+pn-RQRPA [31] (blue). The shaded areas are the currently known-masses region for each element [27], except for the unknown mass of $^{165}_{65}$Tb (red arrow).

FRDM and GT2 are (erratically) out of the data.

RHB+QRPA is more coherent though in few cases also out.

It is important to realize which nuclides are decisive for REE peak formation.

Sensitivity Studies

How do abundances change with change in nuclear inputs?

- ***Baseline simulation*** *– fix conditions & nuclear physics models.*

Produce a final abundance pattern matching reasonably to the main solar pattern A>120.

- ***Modified simulation*** *: change a single piece of nuclear data (say, a single mass or beta-decay rate. Repeat the simulation !*

All the final mass fractions of this simulation X(A) are compared to those of the baseline simulation $X_{baseline}(A)$ making use of

Global Sensitivity Measure

$$F=100\ \Sigma_A\ |X_{baseline}(A)-X(A)|$$

where

$\Sigma A X(A)=1$ *Mass conservation*

$X(A)=AY(A)$ *Mass fraction (X)↔abundance (Y)*

- *The process is repeated for every mass or beta-rate !*
- ***OUTPUT: Sensitivity Measure F for each nucleus in the Network.***

The sensitivity factor F(Z,N) of neutron-rich nuclei with Z=52−70.

$$F(Z,N) = 100 * \sum_{A=150}^{178} |Y^{\uparrow}(Z,N,A) + Y_{\downarrow}(Z,N,A) - 2Y origin(A)|$$

$Y^{\uparrow} \sim 10 * T_{1/2}$

$Y_{\downarrow} \sim 1/10 * T_{1/2}$

Nuclei measured in this work.

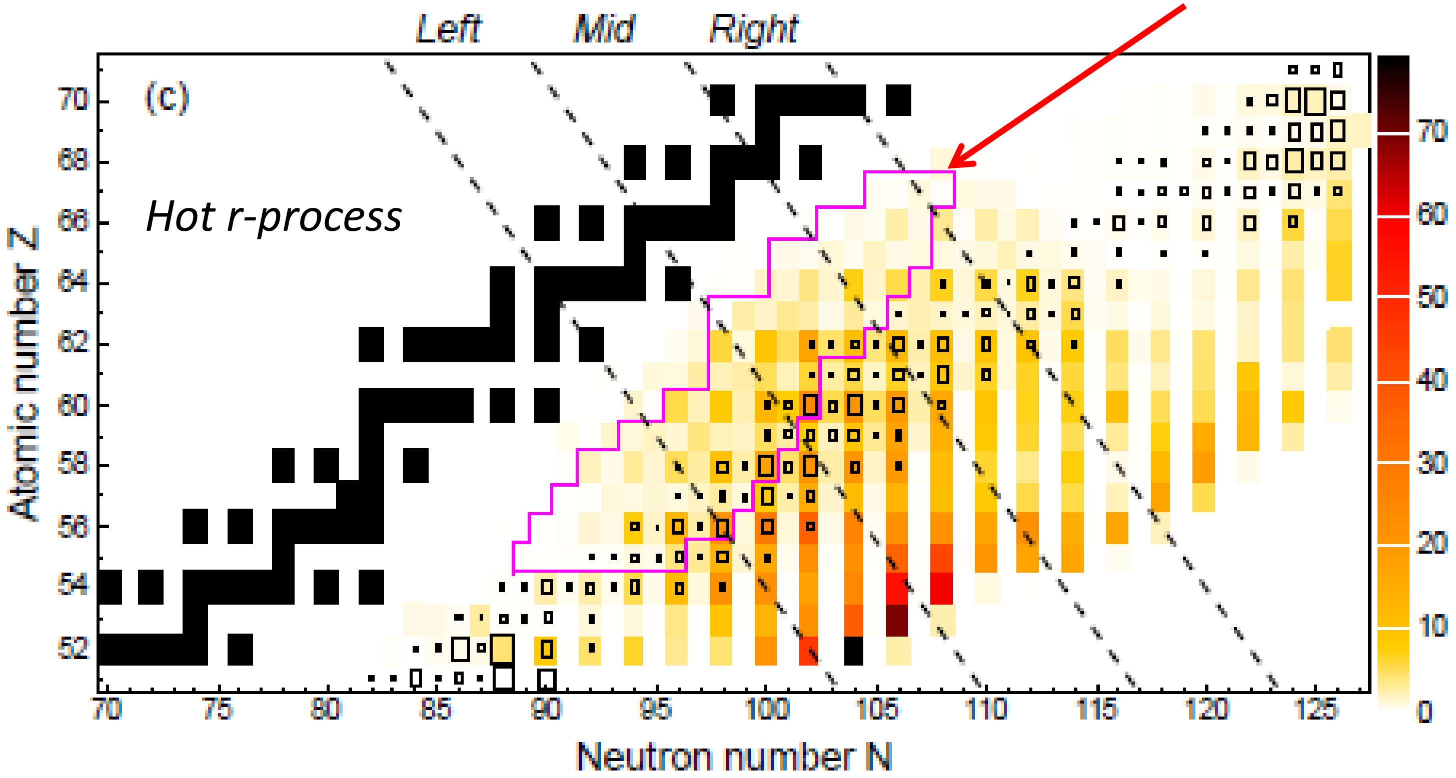

Some important nuclides are still out of reach

The REE peak can be used as a unique probe of the r-process freeze-out conditions and it eventually might help to reveal the currently unknown r-process site.

(a) The r-process abundance pattern observed in the solar system (open circles), Cf. calculated using the **experimental half-lives from this work (black line).**

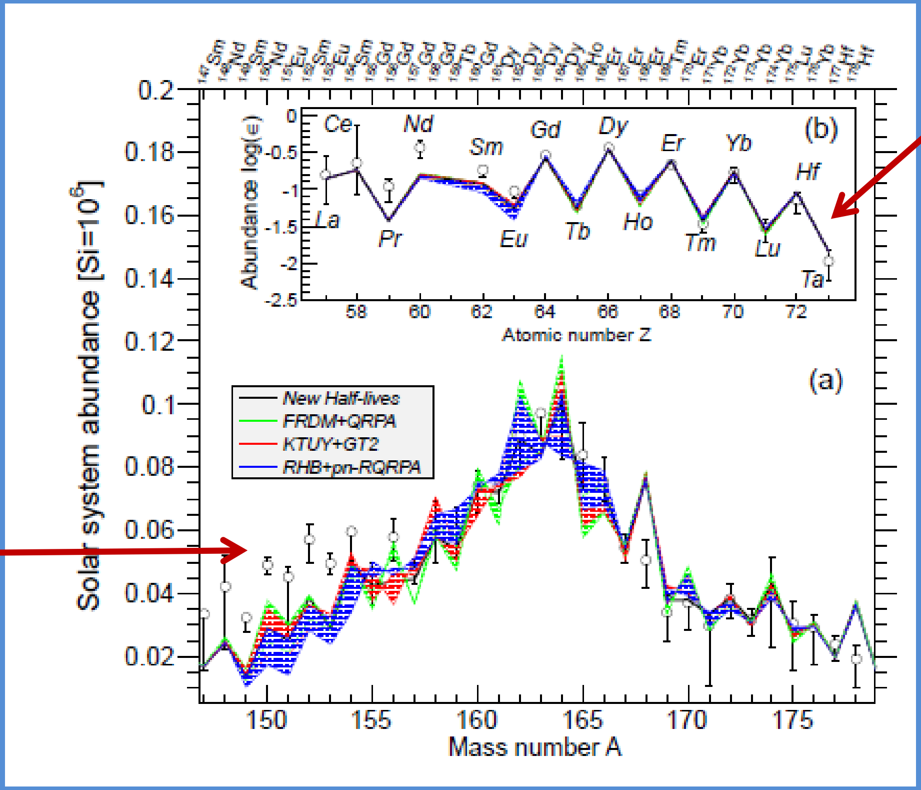

(b) Same as a) but for the elemental abundance pattern compared with one **metal-poor star HD108317.**

The colored areas represent the uncertainty of calculated abundances related to varying by a factor 2 the half-life predictions of the **FRDM+QRPA (green),KTUY+GT2 (red)** and **RHB+pn-RQRPA (blue).**

Changing the astrophysical conditions may change the peak shape but it does not change the relative impact of the half-lives.

T. SHAFER *et al.*

FAM

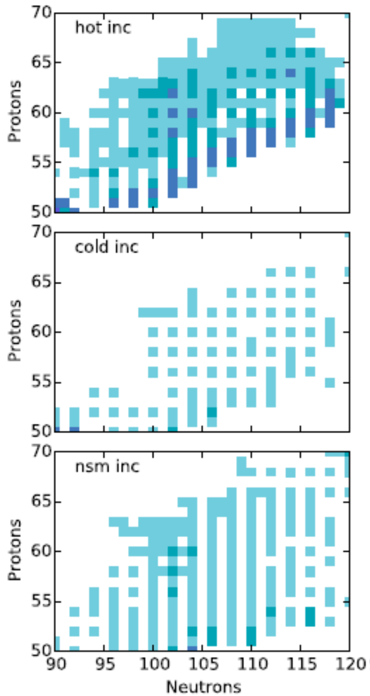

FIG. 2. Influential β-decay rates in the rare-earth region for hot, cold, and merger r-process conditions. The hot conditions are parametrized as in Ref. [50] with entropy $s/k = 200$, dynamical time scale $\tau_{\rm dyn} = 80$ ms, and initial electron fraction $Y_e = 0.3$; the cold conditions are parametrized as in Ref. [51] with $s/k = 150, \tau_{\rm dyn} = 20$ ms, and $Y_e = 0.3$; and the merger conditions are from a simulation of A. Bauswain and H.-Th. Janka, similar to that of Ref. [52]. We performed two sensitivity studies for each trajectory, looking at the results of increases and decreases to the rates by a factor of $K = 5$. In order of lightest to darkest, the shades are white ($f_{\rm local} = 0$), light blue ($0.1 < f_{\rm local} \leqslant 0.5$), medium blue ($0.5 < f_{\rm local} \leqslant 1.0$), dark blue ($1 < f_{\rm local} \leqslant 5$), and darkest blue ($f_{\rm local} > 5$).

In a sensitivity study
70 influential nuclei found (dark blue).

PHYSICAL REVIEW C **94**, 055802 (2016)

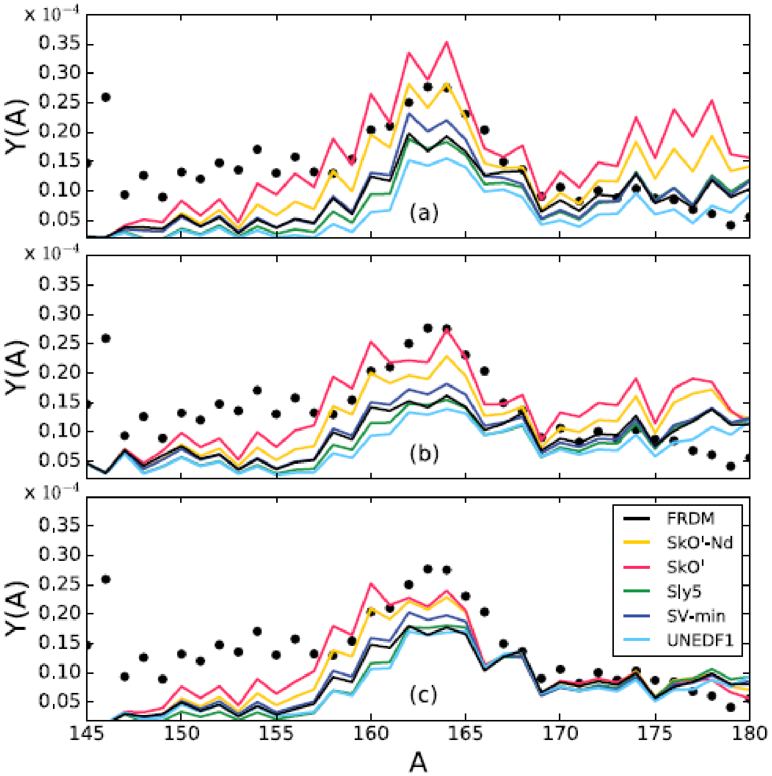

FIG. 14. The effect of our new β-decay rates on final r-process abundances. The same trajectories are used as in Fig. 2: (a) hot, (b) cold, and (c) nsm. Black circles mark solar abundances.

FRDM vs 6 high-end ED-functionals

a,b) Low rates species build up the REE-peak !

c) For NS-NS : low-rate species broaden REEP, shorter-lived – narrow it.

"Hot" vs "cold" r-process

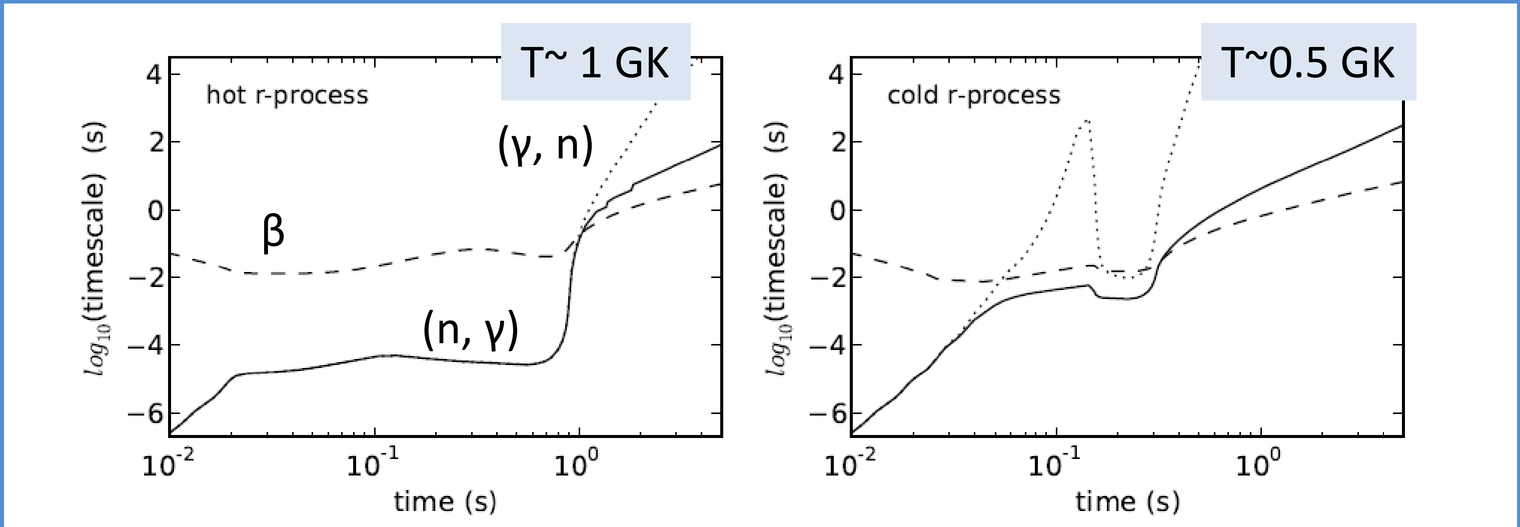

Hot r-process

At T~<3GK: the evolution proceeds under (n, γ) ⇄ (γ, n) equilibrium **with τ(n, γ) = τ(γ,n) ≪ τβ**

It lasts until neutrons are exhausted.
(Here it is at ~ 1 s).
Then beta-decay takes over:
its timescale is getting shorter that 2 others.

Cold r-process

At T<0.5GK: here **τ(n, γ) ≈ τβ ≪ τ(γ,n)!**
(γ,n) is out of game.

The subsequent evolution (here at t>5(-2)s) proceeds via competition solely between **beta decay** and **neutron capture with comparable rates**.

T. Marketin, L. Huther, G. Mart´ınez-Pinedo PRC 93 (2015)

Abundances at the 3rd peak (A~195).
The beta decay half-lives: RHB+CQRPA vs FRDM+RPA

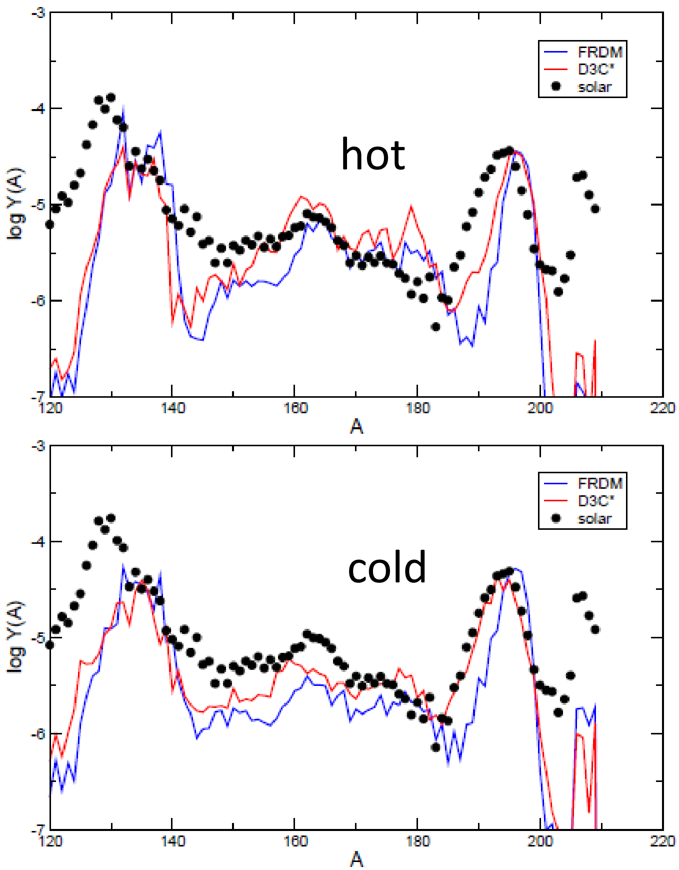

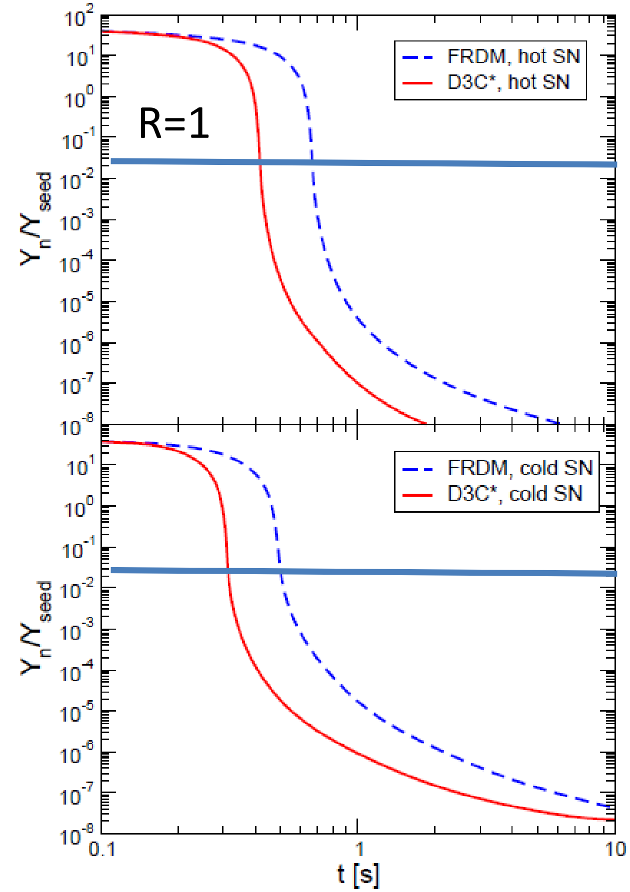

The abundances of heavy nuclei. Hot r-process (upper panel),cold r-process(lower panel). T**he half-lives obtained from the FRDM and the RHB+QRPA. Notice the differences for A=195.**

The evolution of the **neutron-to-seed ratio** during the r-process. The freeze out (R=1) occurs **earlier** for DC3* i.e. at higher density which speeds up it. **Less time for n-captures during the freeze out!**

T. Marketin, L. Huther, G. Mart´ınez-Pinedo PRC 93 (2015)

Faster evolution with new half-lives leads to β-flow equilibrium: $\lambda_\beta(Z)Y(Z) = \text{constant}$

For each Z:

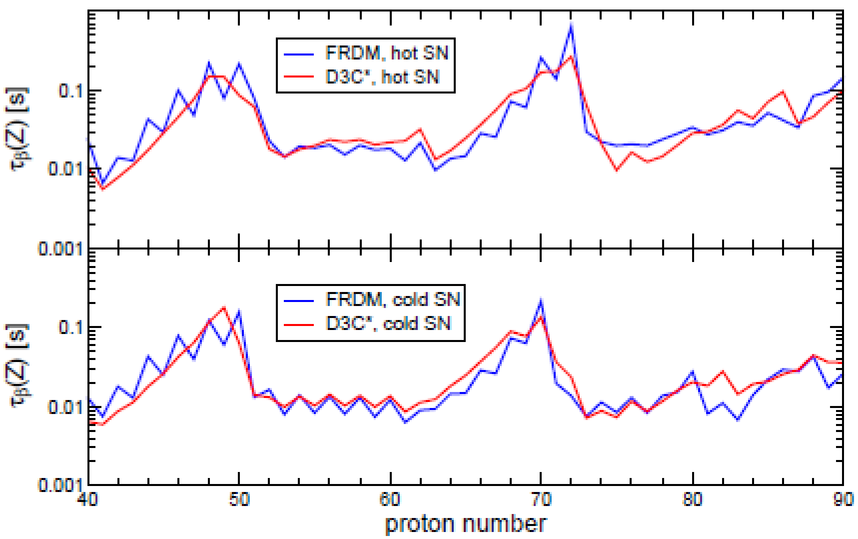

Average beta-rate:

$$\lambda_\beta(Z) = \frac{1}{\tau_\beta(Z)} = \frac{1}{Y(Z)} \sum_A \lambda_\beta(Z,A) Y(Z,A).$$

As Y (Z) are proportional to the lifetime τ(Z), the material accumulates in regions with the longest life-times, namely near the magic shell closures.

The lifetimes are substantially longer for the FRDM+QRPA approach particularly near magic neutron numbers N = 82, corresponding to Z ∼ 50, and N = 126, corresponding to Z ∼ 70.

T. Marketin, L. Huther, G. Mart´ınez-Pinedo PRC 93 (2015)

Conclusion : Nuclear physics uncertainties of r-process nucleosynthesis

The most important nuclear β-decay data in all scenarios of the r-process are

for nuclei near the closed shells N=50, 82,126 as well as in rare earth region (10-20 neutrons away from stability).

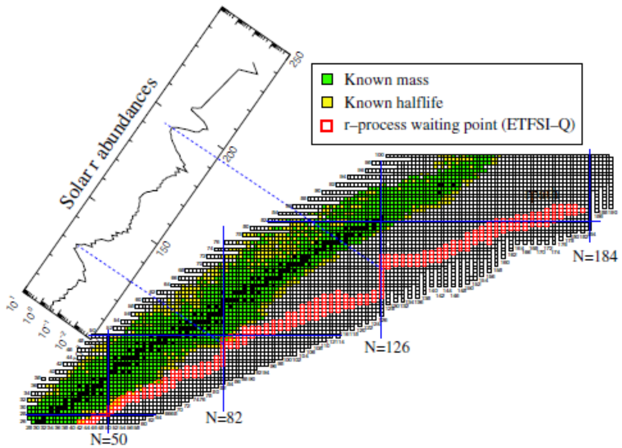

Figure 18. The figure shows the range of r-process paths, defined by their waiting point nuclei. After decay to stability the abundance of the r-process progenitors produce the observed solar r-process abundance distribution. The r-process paths run generally through neutron-rich nuclei with experimentally unknown masses and half lives. In this calculation a mass formula based on the ETFSI model and special treatment of shell quenching [79] has been adopted (courtesy of Kratz and Schatz).

These nuclei can be recommended as targets for acting RIB facilities.

Improved theoretical predictions are welcome!

Российский научный фонд

The study is partially supported by the Russian Scientific Foundation

60 Years IAEA Atoms for Peace and Development

The IAEA support of participation in the CRP «Development of a Reference Database for Beta-Delayed Neutron Emission» is acknowledged.

First measurement of several β-delayed neutron emitting isotopes beyond N=126

R. Caballero-Folch[1,2], C. Domingo-Pardo[3,*], J. Agramunt[3], A. Algora[3,4], F. Ameil[5], A. Arcones[5], Y. Ayyad[6], J. Benlliure[6], I.N. Borzov[7,8], M. Bowry[9], F. Calviño[1], D. Cano-Ott[10], G. Cortés[1], T. Davinson[11], I. Dillmann[2,5,12], A. Estrade[5,13], A. Evdokimov[5,12], T. Faestermann[14], F. Farinon[5], D. Galaviz[15], A.R. García[10], H. Geissel[5,12], W. Gelletly[9], R. Gernhäuser[14], M.B. Gómez-Hornillos[1], C. Guerrero[16,17], M. Heil[5], C. Hinke[14], R. Knöbel[5], I. Kojouharov[5], J. Kurcewicz[5], N. Kurz[5], Yu. A. Litvinov[5], L. Maier[14], J. Marganiec[18], T. Marketin[19], M. Marta[5,12], T. Martínez[10], G. Martínez-Pinedo[5], F. Montes[20,21], I. Mukha[5], D.R. Napoli[22], C. Nociforo[5], C. Paradela[6], S. Pietri[5], Zs. Podolyák[9], A. Prochazka[5], S. Rice[9], A. Riego[1], B. Rubio[3], H. Schaffner[5], Ch. Scheidenberger[5,12], K. Smith[5,20,21,23,24], E. Sokol[25], K. Steiger[14], B. Sun[5], J.L. Taín[3], M. Takechi[5], D. Testov[25,26], H. Weick[5], E. Wilson[9], J.S. Winfield[5], R. Wood[9], P. Woods[11] and A. Yeremin[25]

Physical Review Letters 117, 012501 (2016)

First applications of the Fayans functional to deformed nuclei

S V Tolokonnikov[1,2], I N Borzov[1,3], M Kortelainen[4,5], Yu S Lutostansky[1] and E E Saperstein[1,6]

Journal of Physics G: Nuclear and Particle Physics, Volume 42, Number 7 , p 075102 (2015)

I.N. Borzov[1,2]

Self-consistent approach to beta decay and delayed neutron emission

Physics of Atomic Nuclei, Volume 79, Issue 6, pp 910–923 (2016)

DELAYED MULTI-NEUTRON EMISSION IN NEUTRON-RICH CA REGION

In Proc. VIII Int.Symposium EXON-2016, 4 -10 Sept. 2016, Kazan, RF.

Physics of Atomic Nuclei   July 2017, (submitted)

A. P. Severyukhin,1,2 N. N. Arsenyev,1 I. N. Borzov,3,1 and E. O. Sushenok1,2

Multi-neutron emission of Cd isotopes

PHYSICAL REVIEW C 95, 034314 (2017)

Acknowledgments

N.A. Arsenyev, A.P. Severyukhin, E.O. Sushenok, V .V. Voronov
BLTP, JINR, Dubna

Yu.S. Lutostansky, E.E. Saperstein, S.V. Tolokonnikov
NRC “Kurchatov Institute”, Moscow

N. Van Giai, J. Margeuron, D. Verney
IPN, Orsay

R. Grzywacz, K. Rykaczewski
UTK, Knoxville, ORNL, Oak Ridge